

Design, Structure–Activity Relationships and in Vivo Characterization of 4-Amino-3-benzimidazol-2-ylhydroquinolin-2-ones: A Novel Class of Receptor Tyrosine Kinase Inhibitors

Paul A. Renhowe,* Sabina Pecchi, Cynthia M. Shafer, Timothy D. Machajewski, Elisa M. Jazan, Clarke Taylor, William Antonios-McCrea, Christopher M. McBride, Kelly Frazier, Marion Wiesmann, Gena R. Lapointe, Paul H. Feucht, Robert L. Warne, Carla C. Heise, Daniel Menezes, Kimberly Aardalen, Helen Ye, Molly He, Vincent Le, Jayesh Vora, Johanna M. Jansen, Mary Ellen Wernette-Hammond, and Alex L. Harris

Novartis Institutes for Biomedical Research, 4560 Horton Street, Emeryville, California 94608-2419

Received June 30, 2008

The inhibition of key receptor tyrosine kinases (RTKs) that are implicated in tumor vasculature formation and maintenance, as well as tumor progression and metastasis, has been a major focus in oncology research over the last several years. Many potent small molecule inhibitors of vascular endothelial growth factor receptor (VEGFR) and platelet-derived growth factor receptor (PDGFR) kinases have been evaluated. More recently, compounds that act through the complex inhibition of multiple kinase targets have been reported and may exhibit improved clinical efficacy. We report herein a series of potent, orally efficacious 4-amino-3-benzimidazol-2-ylhydroquinolin-2-one analogues as inhibitors of VEGF, PDGF, and fibroblast growth factor (FGF) receptor tyrosine kinases. Compounds in this class, such as **5** (TKI258), are reversible ATP-competitive inhibitors of VEGFR-2, FGFR-1, and PDGFR β with IC₅₀ values <0.1 μ M. On the basis of its favorable in vitro and in vivo properties, compound **5** was selected for clinical evaluation and is currently in phase I clinical trials.

Introduction

Angiogenesis and maintenance of newly formed blood vessels are important normal physiological processes that are also utilized by tumors to promote their survival, growth, and metastasis.¹ A subset of growth factors (VEGF^a, FGF, and PDGF) and their receptor tyrosine kinases are key signaling molecules during angiogenesis and vascular maintenance. Not surprisingly, many cancer types secrete these growth factors, which can, in turn, stimulate the surrounding tissues and encourage new blood vessel formation. Among the three growth factors, VEGF is considered most important for both normal and pathological angiogenesis.² In addition, some tumors have been found to overexpress the receptors to VEGF, PDGF, and FGF, which allows them to attain additional growth advantages and promote tumor survival.^{3–5} Therefore, direct antitumor effects may be achievable in these tumors if signaling through the receptors is blocked by ATP competitive small molecules that inhibit tyrosine kinase activity. Recent approvals of VEGFR-2 and PDGFR β inhibiting agents, such as small molecules Sunitinib (Figure 1, **1**, SU11248) and Sorafenib (Figure 1, **2**, BAY43-9006), confirm the attractiveness of targeting these receptors for cancer therapy.^{1,6} In addition, several multitargeted small molecule kinase inhibitors have been developed and are being evaluated in clinical trials.⁷ For example, **3** (ABT-869) is an inhibitor of CSF-1R (colony

stimulating factor-1 receptor), PDGFR β , VEGFR-1, VEGFR-2, and FLT-3 and is in phase I clinical trials for acute myelogenous leukemia (AML) and myelodysplastic syndrome (MDS).⁸ In addition, Axitinib (AG-013736, **4**) is an inhibitor of CSF-1R, VEGFR, and PDGFR and is in phase II clinical studies for solid tumors, including metastatic renal cell carcinoma (RCC).⁹

While embarking on an effort to develop RTK inhibitors, we discovered a class of molecules based on a 3-benzimidazol-2-ylhydroquinolin-2-one scaffold (Figure 2) that potently inhibit VEGF, FGF, and PDGF receptor kinases with IC₅₀ values <0.1 μ M. These compounds were also found to possess attractive pharmacokinetic characteristics and efficacy in several human tumor xenograft models. Herein, we describe our progress from lead discovery and optimization of this new class of compounds through the selection of a molecule, **5** (TKI258, Figure 2), for clinical development.^{10–12}

Chemistry

Multiple synthetic routes for the synthesis of the 3-benzimidazol-2-ylhydroquinolin-2-one scaffold were explored before optimal conditions were developed. The initial method involved the reaction of anthranilic acid esters (**6a** and **6b**) with methyl malonyl chloride. The products (**7a** and **7b**) were then condensed with phenylenediamine at elevated temperatures in the absence of solvent^{13–15} to yield the 4-hydroxy-3-benzimidazol-2-ylhydroquinolin-2-ones (**8a** and **8b**)¹⁶ in low to moderate yields (Scheme 1, a). The synthesis of **8c** started from anthranilonitrile and used the same conditions as for the preparation of **8a** and **8b** to yield the 4-amino-3-benzimidazol-2-ylhydroquinolin-2-one **8c** in poor yield (Scheme 1, a). The formation of the *N*¹,*N*^{1'}-dimethylated analogue **10** was achieved by the reaction of *N*-methylisatoic anhydride **9** and ethyl 2-(1-methyl)benzimidazol-2-ylacetate in the presence of LHMDs in THF (Scheme 1, b), while the 4-unsubstituted analogue (**12**) could be obtained

* To whom correspondence should be addressed. Phone: +1-510-923-4055. Fax: +1-510-923-3360. E-mail: paul.renhowe@novartis.com.

^a Abbreviations: RTKs, receptor tyrosine kinases; VEGFR, vascular endothelial growth factor receptor; PDGFR, platelet-derived growth factor receptor; FGFR, fibroblast growth factor receptor; CSF-1R, colony stimulating factor-1 receptor; AML, acute myelogenous leukemia; MDS, myelodysplastic syndrome; RCC, renal cell carcinoma; HTS, high throughput screening; HMVEC, human vascular endothelial cells; VDW, Van Der Waals; CL, plasma clearance; *V*_{ss}, volume of distribution; MED, minimum effective dose; CR, complete response; PR, partial response; ITD, internal tandem duplication.

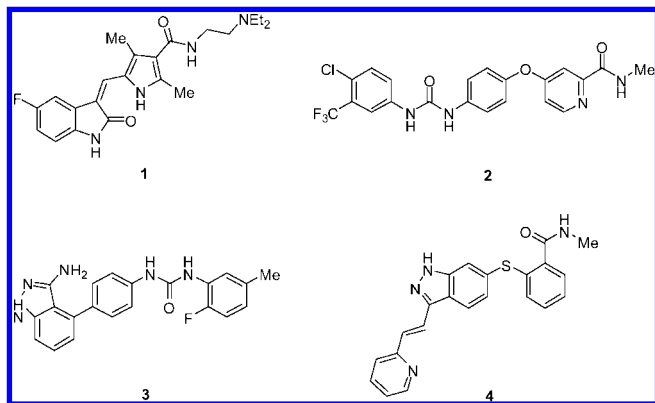


Figure 1. Multikinase Inhibitors.

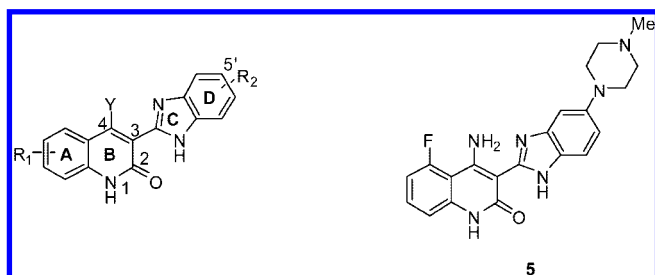
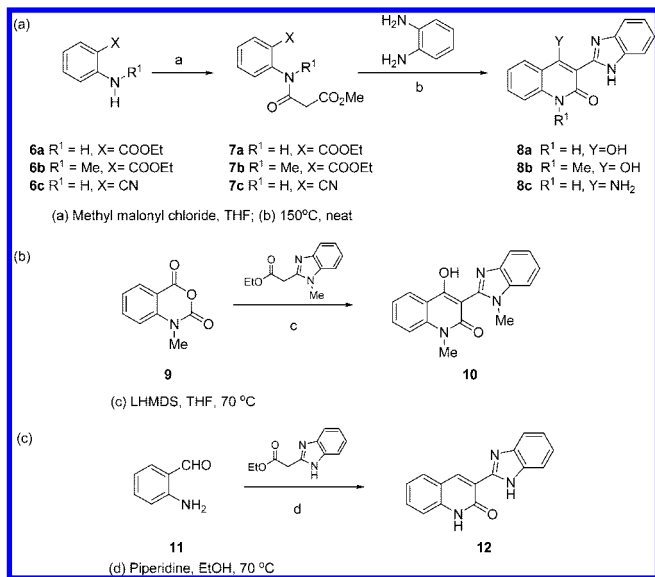


Figure 2. 3-Benzimidazol-2-ylhydroquinolin-2-one Scaffold and 5.

Scheme 1. Syntheses of 3-Benzimidazol-2-ylhydroquinolin-2-one Scaffold



by condensation of 2-aminobenzaldehyde **11** and ethyl 2-benzimidazol-2-ylacetate under Knoevenagel conditions (Scheme 1, c).¹⁷

Examples introducing basic amines at C4 were synthesized as shown in Scheme 2 and previously described.¹⁸ The length of this route and the harsh conditions employed for the removal of the protecting group in the last step made it impractical for compounds bearing a simple NH₂ at C4, in particular when the introduction of substituents on either the A ring or the D ring was required.

A new synthetic route was thus required that was short, amenable to scale up, and tolerant of a variety of functional groups. To this end, the condensation of benzimidazole acetates with anthranilonitriles in the presence of LHMDS in THF was

discovered. This reaction resulted in the formation of the desired 4-amino-3-benzimidazol-2-ylhydroquinolin-2-ones in good yields (Scheme 3),¹⁹ was amenable to multigram scale, and was able to accommodate the presence of many diverse functional groups such as free amines, nitriles, and esters on either the benzimidazole acetate or anthranilonitrile. Worth noting is that the position and nature of R₁ affect the yield of the condensation reaction. When R₁ is ortho to the nitrile and is bulkier than H or F, the formation of the quinolinone ring is much less efficient. For example, the yields of compounds **5** and **19a**, which are substituted at C5, respectively, with a fluorine and hydrogen were 60 and 50%. Compounds **19k** and **19l**, however, which are substituted with a chlorine and methyl at C5, both had significantly lower isolated yields (8%).

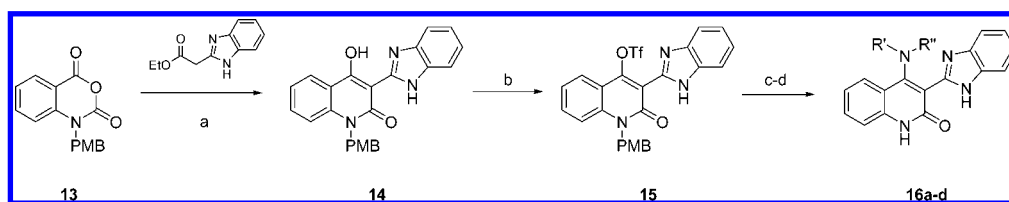
For novel benzimidazoles, the required phenylenediamine could be prepared from commercially available starting materials. For instance, introduction of amino-linked substituents at the 5' site on the benzimidazole ring was achieved by reaction of 2-nitro-5-fluoroaniline with amines at elevated temperatures to yield the 5-amino-2-nitroanilines **21** in high yield and purity (Scheme 4). Ether linked moieties were accessed by reaction of 3-amino-4-nitrophenol with alcohols under Mitsunobu conditions (Scheme 4, b) to give **24**. Reduction of **21** or **24** in the presence of Pd/C and H₂ in EtOH provided the phenylenediamines **22** and **25**, which were used immediately to avoid oxidative decomposition (Scheme 4). The condensation of phenylenediamines with ethyl 3-ethoxy-3-iminopropanoate hydrochloride **20** in EtOH then provided the requisite benzimidazole acetates in good yield (Scheme 4, **23a–d** and **26**).²⁰

The benzimidazole acetates were then reacted with anthranilonitriles in the presence of LHMDS to provide the desired 4-amino-3-benzimidazol-2-ylhydroquinolin-2-ones (Scheme 3). Further modifications could then be carried out as outlined in Scheme 5. For instance, methyl 2-(4-amino-2-oxo-1,2-dihydroquinolin-3-yl)-1H-benzimidazole-5-carboxylate **19ad** could be converted to the piperazinyl amide **19h** or the piperazinyl-methyl analogue **19i** under standard conditions (Scheme 5, a). Furthermore, acylation of the secondary amine **19ah** with bromoacetyl chloride, followed by displacement of the bromine with dimethylamine, gave amide **19j**.

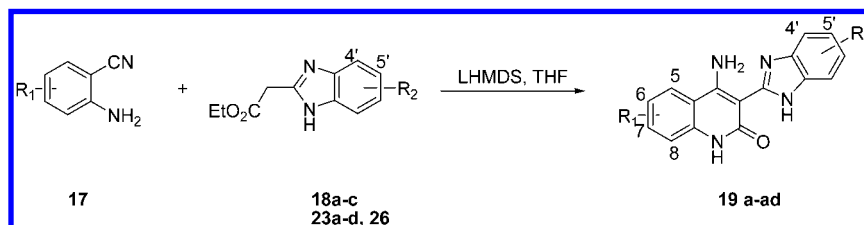
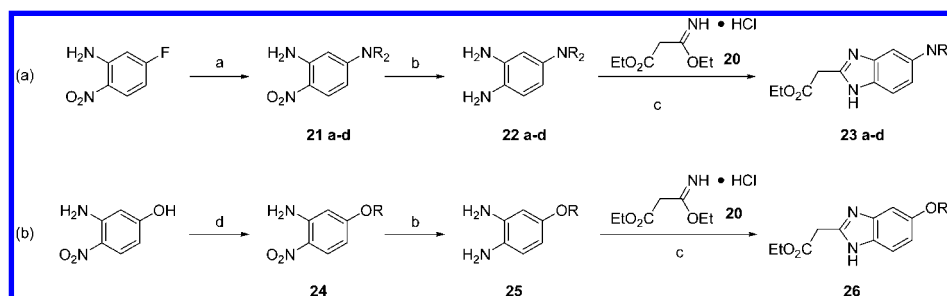
A variety of moieties could also be incorporated into the A-ring of the hydroquinolin-2-one either on the anthranilonitrile starting material or on an advanced 4-amino-3-benzimidazol-2-ylhydroquinolin-2-one intermediate. For instance, amines such as *N*-methylpiperazine could be introduced into the 5- and 6-positions of the hydroquinolin-2-one by synthesizing the appropriate piperazinyl anthranilonitriles **27a** and **27c** according to reported methods (Scheme 6, a and c).^{21,22} The introduction of an ether such as *N*-methylpiperidin-3-yloxy at the 5-position of ring A was achieved by reaction of 3-hydroxy-*N*-methylpiperidine with 2-amino-6-fluorobenzonitrile in the presence of NaH in NMP at 100 °C (Scheme 6, b, **27b**). These modified anthranilonitriles could be carried forward as described in Scheme 3. Other compounds could be synthesized by a late-stage modification, as in the formation of the amide (Scheme 6, reaction d, **19t**). In this case, 4-aminoisophthalonitrile reacted with ethyl 2-[5-(4-methylpiperazinyl)benzimidazol-2-yl]acetate **23b** under the standard LHMDS reaction conditions to give the advanced intermediate **19ai**. The nitrile on the A ring was then hydrolyzed to the carboxylic acid and coupled to benzylamine to give **19t**.

Results and Discussion

Identification of Lead Scaffold and Structure–Activity Relationships. Compound **8a**, a commercially available compound, was identified through high throughput screening (HTS)

Scheme 2. Synthesis of 4-Amino-3-benzimidazol-2-ylhydroquinolin-2-one Scaffold via the Isatoic Anhydride Route^a

^a Reagents and conditions: (a) LHMDS, THF (b) TiF_4 , Pyr (c) $\text{R}'\text{R}''\text{NH}_2$, DIEA; (d) triflic acid, HCl, 80 °C.

Scheme 3. Synthesis of 4-Amino-3-benzimidazol-2-ylhydroquinolin-2-one Scaffold via the LHMDS Route**Scheme 4.** Synthesis of Novel Benzimidazole Acetates^a

^a Reagents and conditions: (a) R_2NH , Et_3N , NMP, 90 °C; (b) H_2 , Pd/c, EtOH; (c) EtOH, 80 °C, (d) ROH, PPh_3 , DIAD, THF.

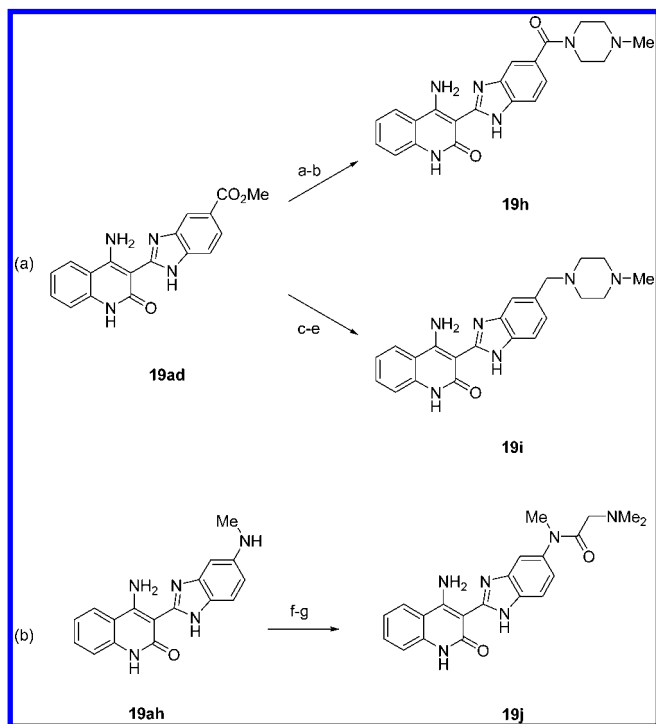
as an inhibitor of VEGFR-2, FGFR-1, and PDGFR β . While the submicromolar activity and low molecular weight of the molecule led us to consider this a good initial hit, it had undesirable physicochemical properties (e.g., solubility) that required further optimization to yield a drug-like compound. Initially, the key structural features required for potent kinase inhibition needed to be determined. Molecular modeling suggested that the NH in position 1 of the hydroquinolin-2-one, the quinolinone carbonyl and the benzimidazole NH formed a donor–acceptor–donor motif that would bind to the hinge region of the RTKs. To test this hypothesis, we systematically masked the hydrogen bond donors by methylation as in **8b**, **8d**, and **10**. These changes led to significant potency loss against all three RTKs, with the dimethylated analogue **10** showing no kinase activity up to 25 μM (Table 1). Interestingly, monomethylation seemed to affect the kinase selectivity profile as well. Introduction of a methyl on the benzimidazole NH (**8d**) had a more dramatic effect on VEGFR-2 affinity than removal of the contact from the NH in position 1 of the hydroquinolin-2-one (**8b**). The effect is opposite for FGFR-1, which indicates that despite the high homology of the two ATP binding sites, selectivity opportunities still exist that are likely due to small changes in the binding site shape, influencing the accessibility of alternate binding poses of the methylated ligands.

Having established the necessity of the donor–acceptor–donor binding motif, the contribution of the C4 hydroxy to the RTK affinity was explored. Removal of the hydroxyl group (**12**) led to significant loss in biochemical potency against VEGFR-2 and FGFR-1; however, cell-based activity in VEGF-driven proliferation of human vascular endothelial cells (HMVEC) was maintained. Replacing the hydroxyl with an unsubstituted amino

group (**8c**) significantly improved RTK affinity and also led to improved cell potency with an EC_{50} of 0.078 μM . The potency decrease observed ($\text{NH}_2 > \text{OH} > \text{H}$) suggests an important role for a hydrogen bond donating group in the C4 position (**8c**, **8a**, and **12**). This observation is further supported by a 4-fold decrease in potency when a methylamino group (**16a**) is replaced with a dimethylamino group (**16b**). However, this loss in RTK affinity is not as dramatic as the loss caused by masking one of the hydrogen bonds in the donor–acceptor–donor motif, which interacts with the hinge region. One hypothesis to explain this more subtle effect is that the hydrogen on the C4 substituent is needed to stabilize the benzimidazole tautomer such that the hydrogen bond donating moiety points toward the hinge and presents the full donor–acceptor–donor motif.

Once the basic structural components needed for affinity to our targets of interest were understood, a study of the structure–activity relationship around the periphery of the scaffold was undertaken together with the incorporation of moieties that might impart favorable physicochemical properties. Thus, incorporation of larger substituents on the C4 NH of the hydroquinolin-2-one was explored and found to be tolerated (**16a–d**). When the substituent carried an additional basic nitrogen, solubility was improved.²³ More importantly, it was discovered that this position was useful in modulating the selectivity profile of this class of compounds among the RTKs. For instance, both **16c** and **16d** are more potent against PDGFR than VEGFR-1 (3000-fold) and FGFR (>1500-fold), with similar trends seen against other kinases as well. In particular, incorporation of a large basic amine such as an aminoquinclidine as in **16c** led to very potent CHK-1 and GSK-3 inhibitors.¹⁸ For our RTK inhibitor program, however, the NH_2

Scheme 5. Late Stage Modifications to the 4-Amino-3-benzimidazol-2-ylhydroquinolin-2-one Core^a



^a Reagents and conditions: (a) EtOH, KOH; (b) *N*-methylpiperazine, EDCI, HOAT, Et₃N, DMF; (c) DIBAL-H, PhMe; (d) MnO₂, DMA; (e) *N*-methylpiperazine, Na(OAc)₃BH, DMA; (f) bromoacetyl chloride, DMA, Et₃N; (g) dimethylamine, EtOH.

group was the optimal substituent at C4 as it avoided inhibition of these additional serine threonine kinases, which could complicate the pharmacological application of these agents. The NH₂ substitution at C4 was thus maintained, and subsequent efforts focused on modifying the A and D rings to attain additional enzymatic affinity and to improve physicochemical properties.

Initially, small groups such as methyl were appended to the D ring and were generally tolerated (**19a**–**19b**, Table 2). The major goal for this series was to improve solubility. In fact, the poor physicochemical properties of the early compounds prevented us from obtaining a meaningful pharmacokinetic profile as a suitable formulation for in vivo dosing could not be found. To this end, a number of solubilizing groups was explored (**19c**–**19j**). It was found that C5' tolerated a variety of substituents including amines (**19c**–**19f**), ethers (**19g**), amides (**19h** and **19j**), and methylene extended amines (**19i**) without significant variations in in vitro potency. Carboxylic acid, ester, and nitrile C5' substitutions were also tolerated.²⁴ Varying the substituent in this position did not affect the selectivity profile, suggesting that this substituent is most likely solvent exposed. A basic amine with a pK_a in the range of 7–9 on the C5' substituent (as in **19d**–**19j**) improved the cellular potency 2-fold.

As the C5' 1-methylpiperazine moiety afforded a potent compound (**19d**) with adequate solubility and in vivo properties, 1-methylpiperazine was selected as the default D ring substituent for A ring SAR (Table 3). Small, electronegative substituents such as fluorine are tolerated at C5 (**5**), C6 (**19n**), and C7 (**19u**) of ring A. However, a fluorine substituent at C8 (**19w**) as well as difluoro substitution (**19x** and **19y**) resulted in a degradation of affinity. Introducing a chlorine (**19k**) or methyl (**19l**) at C5 slightly improves affinity, whereas C5-methylamino (**19m**) retains affinity compared to **19d**. Incorporation of substituents

at C6 such as chlorine (**19o**) and a primary amine (**19p**) preserves activity, however, a dimethylamino group at this position (**19q**) shows a slight drop in affinity with a complete loss of cell-based potency. At C6, some aromatic substituents caused no change in affinity (**19s** and **19t**) while others did (**19r**) depending on the length and flexibility of the linker to the scaffold. In spite of the fact that the biochemical potency for compounds **19s** and **19t** is similar to the unsubstituted example (**19d**), the cell potency loss is significant. This may be a function of a difference in cell permeability and access to the relevant subcellular compartments; however, no data were collected to determine the above parameters.²⁵ At C7, any substituent larger than a fluorine led to significant decrease in potency against all targets (**19v** and **19z**).

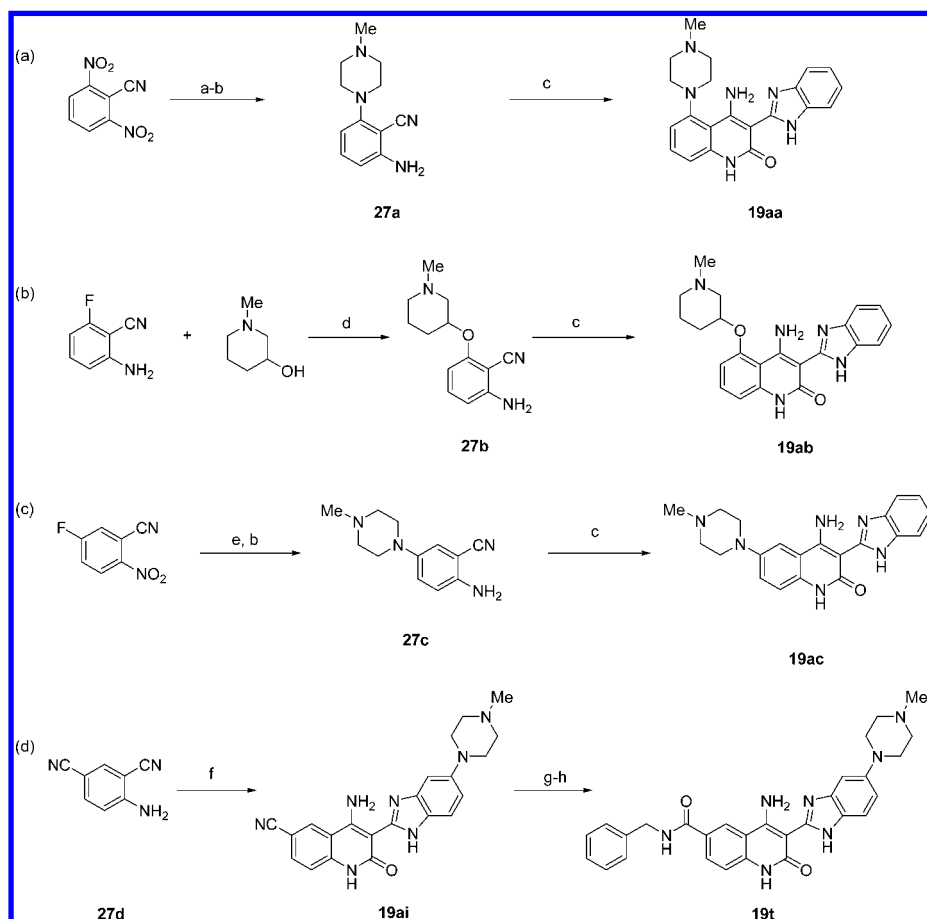
To finish exploring the SAR of the A ring, a number of solubilizing groups at the C5 and C6 positions were incorporated (Table 4). At C5, groups such as piperazine (**19aa**) and 1-methylpiperidin-3-ol (**19ab**) yielded highly potent analogues. The cellular potency for **19aa** decreased, but for **19ab**, the cellular potency was retained. Finally, adding a piperazine at C6 (**19ac**) led to significant loss of affinity for VEGFR-2 and FGFR-1.

Many of the compounds highlighted in this paper show greater in vitro potency against PDGFR β than VEGFR-2 or FGFR-1. However, for **5**, biochemical inhibition of VEGFR-2, FGFR-1, and PDGFR β translated into comparable EC₅₀s for inhibition of VEGFR-2 and PDGFR β phosphorylation (0.046 and 0.051 μ M) and 3-fold less potent inhibition of FGFR-1 phosphorylation in cells (0.166 μ M).^{10,12}

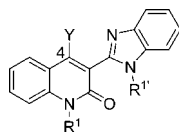
The culmination of the medicinal chemistry effort led to the selection of compound **5** as a candidate for further development. Compound **5** has high potency not only against VEGFR-2, FGFR-1, and PDGFR β but also against VEGFR-1/3, FGFR-3, c-Kit, CSF-1R, and FLT-3 enzymes (IC₅₀ values between 3 and 27 nM), which translates to inhibition of VEGF-, FGF-, SCF-, CSF-, and PDGF-mediated cell proliferation and induction of apoptosis in specific cancer cell lines.^{10–12} The antiproliferative effect of **5** corresponded with reduction of VEGF-mediated KDR/VEGFR-2 and ERK phosphorylation in endothelial cells.²⁶ In summary, **5** inhibits multiple growth factor receptor tyrosine kinases that are important for tumor angiogenesis and tumor growth.

Molecular Modeling. VEGFR-2 binding site models for the 4-amino-3-benzimidazol-2-ylhydroquinolin-2-one based inhibitors described herein were developed using a homology model based on the FGFR-1 crystal structure (PDB access code 2FGI)²⁷ and optimized using the observed SAR as well as crystal structure data for a compound with the same core in CHK-1.¹⁸ The conformation of the activation loop in the FGFR-1 template has the highly conserved Asp-Phe-Gly (or DFG) motif in the active and so-called “in” conformation in which the phenylalanine packs under helix C and fits in an internal hydrophobic pocket. Inactive kinase structures have been crystallized where the DFG motif adopts a radically different conformation, which perturbs the catalytically active orientation of the activation loop and helix C and moves the phenylalanine of the DFG-motif “out” of its pocket, leaving it available for occupancy by inhibitors.²⁸

The choice for the DFG-in conformation as a template was based on the fact that the current series of inhibitors does not seem to extend far enough into the phosphate binding region to induce the DFG-out conformational shift. It is quite possible that the protein exhibits a conformational equilibrium between DFG-in and DFG-out conformations while bound to these

Scheme 6. Synthesis of Ring A Substituted 4-Amino-3-benzimidazol-2-ylhydroquinolin-2-ones^a

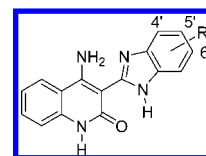
^a Reagents and conditions: (a) *N*-methylpiperazine, DMF, 90°C; (b) H₂, Pd/C, EtOH; (c) ethyl 2-benzimidazol-2-ylacetate, LHMDs, THF; (d) NaH, NMP, 100°C; (e) *N*-methylpiperazine, Et₃N, NMP, 50°C; (f) 23b, LHMDs, THF; (g) NaOH, EtOH, 100°C; (h) benzylamine, EDCI, HOAT, Et₃N, DMF.

Table 1. Structure–Activity Relationships at C4

Compound	Y	R ¹	R ^{1'}	VEGFR-2 IC ₅₀ (μM)	FGFR-1 IC ₅₀ (μM)	PDGFRβ IC ₅₀ (μM)	HMVEC EC ₅₀ (μM)
8a	OH	H	H	0.24	0.090	0.020	0.42
8b	OH	Me	H	5.8	>25	19	4.6
8d	OH	H	Me	>25	7.9	1.1	>10
10	OH	Me	Me	>25	>25	>25	>10
12	H	H	H	1.7	0.39	0.070	0.24
8c	NH ₂	H	H	0.058	0.030	0.010	0.078
16a	NHMe	H	H	0.22	0.12	0.030	0.28
16b	NMe ₂	H	H	0.86	0.39	0.070	>10
16c		H	H	0.17	0.19	0.0002	0.072
16d		H	H	0.94	0.55	0.0009	0.10

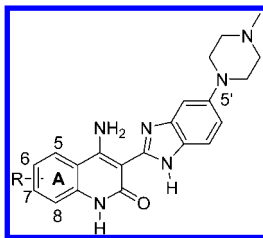
inhibitors,²⁹ but for the purposes of understanding SAR from a structural perspective, the DFG-in conformation seems most appropriate.

The model derived for **5** is shown in Figure 3. The interactions with the modeled active site include an optimal set of three hydrogen bonds to the hinge domain (Glu917 and Cys919). The

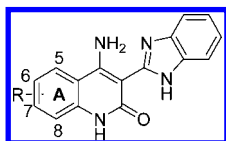
Table 2. Structure–Activity Relationships Around Ring D

Compound	R ^{4'}	R ^{5'}	R ^{6'}	VEGFR-2 IC ₅₀ (μM)	FGFR-1 IC ₅₀ (μM)	PDGFRβ IC ₅₀ (μM)	HMVEC EC ₅₀ (μM)
8c	H	H	H	0.058	0.030	0.010	0.078
19a	H	Me	H	0.22	0.080	0.030	0.064
19b	H	Me	Me	0.21	0.070	0.012	0.15
19c	H		H	0.057	0.030	0.005	0.051
19d	H		H	0.042	0.009	0.002	0.019
19e	H		H	0.066	0.020	0.005	0.025
19f	H		H	0.060	0.020	0.004	0.042
19g	H		H	0.066	0.020	0.005	0.037
19h	H		H	0.026	0.010	0.0009	0.045
19i	H		H	0.027	0.009	0.002	-
19j	H		H	0.029	0.003	0.001	0.024

A-ring makes good Van Der Waals (VDW) contacts to the gatekeeper residue, Val916, and is in addition well-positioned

Table 3. Structure–Activity Relationships around Ring A

compd	R ⁵	R ⁶	R ⁷	R ⁸	VEGFR-2 IC ₅₀ (μM)	FGFR-1 IC ₅₀ (μM)	PDGFRβ IC ₅₀ (μM)	HMVEC EC ₅₀ (μM)
19d	H	H	H	H	0.042	0.009	0.002	0.019
5	F	H	H	H	0.065	0.011	0.005	0.013
19k	Cl	H	H	H	0.014	0.002	0.0003	0.012
19l	Me	H	H	H	0.012	0.003	0.0007	0.005
19m	MeNH	H	H	H	0.053	0.015	0.002	0.017
19n	H	F	H	H	0.078	0.040	0.001	0.010
19o	H	Cl	H	H	0.043	0.024	0.008	0.039
19p	H	NH ₂	H	H	0.019	0.007	0.007	0.017
19q	H	Me ₂ N	H	H	0.16	0.083	0.007	2
19r	H	PhC(O)NH	H	H	0.98	0.90	0.039	-
19s	H	BnNH	H	H	0.021	0.008	0.0006	1.1
19t	H	BnNHC(O)	H	H	0.050	0.010	0.0001	0.12
19u	H	H	F	H	0.014	0.003	0.0004	0.034
19v	H	H	MeNH	H	1.0	0.37	0.009	0.27
19w	H	H	H	F	0.56	0.19	0.014	0.42
19x	H	F	F	H	0.19	0.11	0.003	0.48
19y	F	H	F	H	0.13	0.030	0.005	0.080
19z	H	F	Me ₂ N	H	5.3	1.8	0.030	3.3

Table 4. Incorporation of Solubilizing Groups on Ring A

Compound	R ⁵	R ⁶	VEGFR-2 IC ₅₀ (μM)	FGFR-1 IC ₅₀ (μM)	PDGFRβ IC ₅₀ (μM)	HMVEC EC ₅₀ (μM)
8c	H	H	0.058	0.030	0.010	0.078
19aa		H	0.017	0.001	0.0003	0.34
19ab		H	0.005	0.001	0.0001	0.010
19ac	H		6.5	4.1	0.13	-

to engage in an S–H/π interaction with Cys1045. This is a similar interaction as described for a newly designed FLT-3 kinase inhibitor³⁰ and involves the residue preceding the DFG-motif. Residues engaged in favorable VDW contacts with the ligand are Leu840, Val848 (both in the P-loop and ceiling of the purine pocket), Ala866 (ceiling of the purine pocket), Val 899 (floor of the purine pocket), Phe918 (part of the hinge), Lys920, Gly922 (both in the lower hinge region), and Leu1035 (floor of the purine pocket).

To validate this binding mode model, the SAR described above is evaluated in context of the model. The 7- and 8-positions of the core are in close contact with the gatekeeper residue (Val916), while the 8-position is also in VDW contact with the hinge (Glu917). This snug fit explains why not even F-substitution is allowed at the 8-position, and at the 7-position, nothing bigger than F seems to be tolerated without effecting affinity. The 6-position has a vector pointing into available space, supported by the observation of various high affinity

6-substituted analogues like **19t**. The C6-vector does point toward the catalytic Lys868, which may be why the rigid C6-piperazine analogue (**19ac**) has highly reduced affinity. The reduced affinity for the C6-dimethyl-amino compound (**19q**) is hypothesized to be due to a clash of one of the methyl groups with the Lys868/ Glu885 salt-bridge. The benzyl-amide analogue **19t** would experience a similar steric clash, but the C=O functionality in the ligand might induce a conformational change in the protein to allow a hydrogen bond between the C=O and the side chain of Lys868. The vector available for substitution on C5 is pointing into the biggest area of available space, which is supported by the good affinity for all 5-substituted analogues. Finally, substituting the C5' position has little effect on potency or selectivity, which is in agreement with this model where substituents on that position are solvent-exposed and the kinases in our panel are expected to have comparable solvent access from the ATP binding site.

Pharmacokinetic Profile. Once solubility was improved, the attractive pharmacokinetic properties of the scaffold were apparent. The single dose pharmacokinetics of **5** were studied in mice and rats, and the summary of PK parameters is presented in Table 5.³¹ In both species, oral bioavailability was high (>70%). After intravenous injection, **5** exhibited moderate to high plasma clearance (CL) relative to liver plasma flow, a large volume of distribution (*V*_{ss}) and was eliminated with a terminal half-life (*t*_{1/2}) of approximately 3 h.

In Vivo Pharmacology of 5 in Preclinical Models. Dose–response effects of **5** were examined for potency in preclinical models of angiogenesis and specific target-driven cancers. The murine Matrigel model of bFGF-induced neovascularization was used to evaluate the effects of **5** on in vivo angiogenesis. Supplementation with bFGF induces blood vessel formation in Matrigel implants that was quantified by measuring the amount of hemoglobin in Matrigel plugs following removal from animals (Figure 4). Compound **5** administered orally at doses from 3 to 300 mg/kg for 8 days demonstrated a dose-

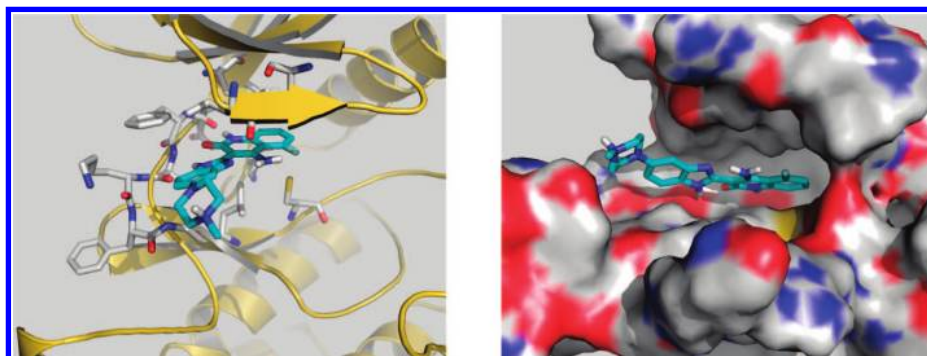


Figure 3. Binding site model for compound **5** in the VEGFR-2 homology model. (a) Cartoon representation of the kinase with residues interacting with the ligand in stick model. (b) Surface representation, with the surface colored by atom type (red = oxygen, blue = nitrogen, yellow = sulfur, gray = carbon/hydrogen). The donor–acceptor–donor motif is shown to interact with the hinge region while the 1-methylpiperazine substituent on C5' points into solution.

Table 5. Summary of Plasma Pharmacokinetic Parameters of **5**^a

species	dose (mg/kg)	%F ^b	C _{max} (ng/mL) ^b	AUC (ng·min/mL) ^b	CL (mL/min/kg) ^c	V _{ss} (mL/kg) ^c	t _{1/2} (h) ^c
mouse	5 (IV)/20 (PO)	77	670	360000	42	12000	2.7
rat	5 (IV)/20 (PO)	73	480	340000	43	13000	3.5

^a CL, clearance; F, oral bioavailability; t_{1/2}, half-life; V_{ss}, volume of distribution. ^b Determined from the oral data. ^c Determined from the intravenous data.

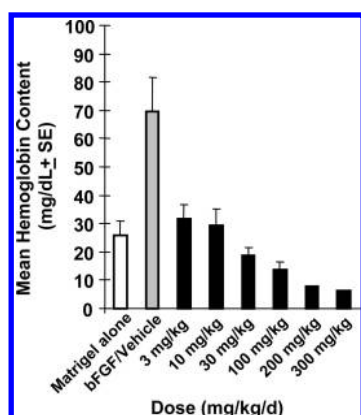


Figure 4. Treatment with **5** inhibits angiogenesis in a bFGF-induced Matrigel model in vivo. Matrigel containing bFGF was injected subcutaneously into mice, and **5** was administered orally for 8 days (0–200 mg/kg/d). The Matrigel plugs were removed, and hemoglobin concentration was measured (*n* = 8 mice/group).

dependent inhibition of angiogenesis with a calculated ED₅₀ of 3 mg/kg (Figure 4). Substantial antiangiogenic activity with **5** was observed at 3 mg/kg/d (54%, *p* = 0.01), indicating potent inhibition of bFGF-driven angiogenesis in vivo.

The efficacy of **5** was examined in three subcutaneous human xenograft tumor models, KM12L4A (colon), DU145 (prostate), and MV4;11 (AML) (Table 6). In efficacy studies, mice with subcutaneous tumors were randomized at a mean size of 200–500 mm³, and treatments of vehicle or **5** were administered daily by oral gavage. Dose response effects and statistically significant tumor growth inhibition were observed in all three models tested, with disease stabilization and some tumor regressions occurring at 100 mg/kg/d dose level (Table 6). The minimum effective dose (MED) for KM12L4A (expressing VEGFR and PDGFRβ) and DU145 (expressing VEGFR, FGFR, and PDGFRβ) were 10 mg/kg/d and 30 mg/kg/d, respectively, and the corresponding calculated ED₅₀'s were 17 and 23 mg/kg/d, respectively. In comparison, in the MV4;11 xenograft tumor model, driven by FLT-3 ITD mutations, potent tumor growth inhibition was observed at doses of ≥ 1 mg/kg/d with a MED of 1 mg/kg/d. Pertinently, in this target-driven FLT-3 ITD MV4;11 model, significantly lower ED₅₀s (3 mg/kg/d vs 17–23 mg/kg/d in KM12L4A or DU145) and significantly higher numbers of responses (both CR and PR) were observed at doses ≥ 10 mg/kg/d.

Conclusion

In conclusion, the 4-amino-3-benzimidazol-2-ylhydroquinolin-2-one series represents a novel scaffold with multikinase

Table 6. Efficacy of **5** in Tumor Xenograft Models in Vivo^a

tumor model (cancer type)	target RTKs expressed	TGI ^b (dose, mg/kg/d; tumor responses ^c)	MED (mg/kg/d) ^e	ED ₅₀ (mg/kg/d) ^d
KM12L4A (colon)	VEGFR PDGFRβ	44% (10; 0 CR/PR) 55% (30; 0 CR/PR) 95% (100; 1CR, 3PR)	10	17
DU145 (prostate)	VEGFR PDGFRβ FGFR	39% (10; 0 CR/PR) 70% (30; 0 CR/PR) 86% (100; 1PR)	30	23
MV4;11 (AML)	FLT-3 ITD VEGFR cKIT PDGFRβ FGFR	23% (1; 0 CR/PR) 65% (5; 0 CR/PR) 92% (10; 1CR, 5PR) 96% (30; 1CR, 8PR)	1	3

^a Subcutaneous KM12L4A, HCT-116, DU145, or MV4;11 tumors in nude or SCID-NOD mice (size of 200–500 mm³, 10/group) were treated with daily oral administration of either vehicle or **5**. RTK, receptor tyrosine kinase; ITD, internal tandem duplication. ^b Tumor growth inhibition (TGI) was calculated as [1 – (mean tumor volume of treated group/mean tumor volume of control group) × 100], when mean of vehicle tumors were ~1000–2000 mm³, KM12L4A (day 9); DU145 (day 22); MV4;11 (day 15). ^c Tumor responses were defined as either complete (no measurable tumor; CR), or partial (50–99% tumor volume reduction; PR) compared to tumor volume for each animal at treatment initiation. ^d MED = minimum effective dose; lowest dose that is statistically different vs vehicle treatment. ^e ED₅₀ = dose of test agent producing 50% TGI.

affinity. These compounds inhibit RTKs such as VEGFR-2, FGFR-1, PDGFR β , and FLT-3, possess good pharmacokinetic and pharmacological characteristics, and are well tolerated. They may find application in the treatment of solid and hematological malignancies, acting not only as antiangiogenic agents but also affecting tumors in which the above pathways are deregulated and contribute to tumorigenesis. Among all compounds surveyed, **5** was selected to advance to development, based on its favorable in vitro potency, drug-like properties, and attractive pharmacological and toxicological profiles. Compound **5** is currently in phase I clinical trials.

Experimental Section

Chemistry. ^1H and ^{13}C NMR spectra of all compounds were recorded at 300 and 75 MHz, respectively. ^1H shifts are referenced to the residual protonated solvent signal (δ 2.50 for DMSO- d_6), and ^{13}C shifts are referenced to the deuterated solvent signal (δ 39.5 for DMSO- d_6). ^{13}C multiplicities were deduced from DEPT or APT experiments. Mass spectrometric analysis was performed on one of two LCMS instruments: a Waters system (Alliance HT HPLC and a Micromass ZQ mass spectrometer; column: Eclipse XDB-C18, 2.1 mm \times 50 mm; solvent system: 5–95% acetonitrile in water with 0.1% TFA; flow rate: 0.8 mL/min; molecular weight range: 150–850; cone voltage: 20 V; column temperature 40 $^\circ\text{C}$) or a Hewlett-Packard system (Series 1100 HPLC; column: Eclipse XDB-C18, 2.1 mm \times 50 mm; solvent system: 5–95% acetonitrile in water with 0.1% TFA; flow rate: 0.8 mL/min; molecular weight range: 150–850; cone voltage: 50 V; column temperature 30 $^\circ\text{C}$). All masses were reported as those of the protonated parent ions.

The following compounds were commercially available: 2-aminobenzonitrile (Aldrich), 2-amino-5-chlorobenzonitrile (Aldrich), 2-amino-5-fluorobenzonitrile (Aldrich), 2-amino-6-chlorobenzonitrile (Alfa Aesar), 2,5-diaminobenzonitrile (Apin), 2-amino-6-methylbenzonitrile (Fluka), **8a** and **8b** (Aurora Screening Library). The synthesis of 2-amino-5-(dimethylamino)benzonitrile,³² 2-amino-4-fluorobenzonitrile,³³ have previously been described. ^1H and ^{13}C NMR spectra of the 4-amino-3-benzimidazol-2-yl hydroquinolin-2-ones were recorded on the hydrochloride salts, except for **12**, which was recorded as the free base and **5**, which was recorded as the sulfate salt. Elemental analyses were performed on free base.

4-Hydroxy-1-methyl-3-(1-methyl-1H-benzo[d]imidazol-2-yl)quinolin-2(1H)-one (10). To a solution of ethyl 2-(1-methyl)-benzimidazol-2-ylacetate (122 mg, 0.56 mmol, 1.0 equiv) in a mixture of anhydrous THF at -78 $^\circ\text{C}$ under an atmosphere of nitrogen was added LHMDs (1 M in THF, 0.85 mL, 1.5 equiv). After 1 h, a solution of 1-methylbenzo[d]1,3-oxazaperhydroine-2,4-dione **9** (100 mg, 0.56 mmol, 1.0 equiv) in anhydrous THF was added dropwise, and the resulting mixture was allowed to warm to room temperature and stirred overnight. The reaction was then quenched with NH_4Cl (aq. sat.), and the aqueous layer was extracted with CH_2Cl_2 (4 \times). The combined organic layers were dried over Na_2SO_4 and concentrated in vacuo, and the resulting crude material was purified by column chromatography on silica gel to afford **10** (30 mg, 20% yield) as an off-white solid. ^1H NMR (300 MHz, DMSO- d_6) 8.16 (1 H, dd, J = 7.8, 1.5 Hz), 7.96 (1 H, m), 7.81 (1 H, m), 7.73 (1 H, m), 7.57 (3H, m), 7.30 (1 H, dd, J = 8.1, 7.2 Hz), 3.85 (3 H, s), 3.60 (3 H, s). LCMS (m/z) 306 (MH^+), R_t 1.95 min.

3-Benzimidazol-2-ylhydroquinolin-2-one (12). 2-Aminobenzaldehyde **11** (180 mg, 1.47 mmol, 1.0 equiv) and ethyl 2-benzimidazol-2-ylacetate (300 mg, 1.47 mmol, 1.0 equiv) were dissolved in EtOH (6 mL). Piperidine (0.150 mL, 1.29 mmol, 1.0 equiv) was added, and the solution was heated at 70 $^\circ\text{C}$ overnight. A precipitate formed, which was filtered. The solid was washed with EtOH and dried to obtain **12** (300 mg, 78% yield) as bright-yellow needles. ^1H NMR (300 MHz, DMSO- d_6) 12.65 (1 H, s, NH), 12.47 (1 H, s, NH), 9.11 (1 H, s), 7.95 (1 H, d, J = 7.8 Hz), 7.70 (2 H, bs), 7.61 (1 H, dd, J = 8.1, 7.2 Hz), 7.44 (1 H, d, J = 8.1 Hz), 7.27 (1 H, dd, J = 7.8, 7.2 Hz), 7.20 (2 H, m). ^{13}C NMR (75

MHz, DMSO- d_6) 160.8, 147.7, 142.8, 138.1, 138.7, 134.4, 131.6, 129.0, 122.6, 122.1 (2 Cs), 120.0, 119.1, 118.3, 115.2, 112.8. LCMS (m/z) 262.2 (MH^+), R_t 1.88 min. HRMS found m/z 262.0974; $\text{C}_{16}\text{H}_{12}\text{N}_3\text{O}$ requires 262.0981. Anal. calcd for $\text{C}_{16}\text{H}_{11}\text{N}_3\text{O}$: C 73.55 H 4.24, N 16.08; found: C 70.79, H 3.95, N 15.28.

4-amino-3-(1H-benzo[d]imidazol-2-yl)quinolin-2(1H)-one (8c). To 2-aminobenzonitrile **6c** (0.1 g, 0.85 mmol, 1.0 equiv) in CH_2Cl_2 (5 mL) was added sequentially Et_3N (0.36 mL, 2.55 mmol, 3.0 equiv) and methyl malonylchloride (0.11 mL, 1.02 mmol, 1.2 equiv). The reaction was stirred at room temperature for 30 min, upon which starting materials had been consumed as monitored by LCMS. The reaction was quenched with NaHCO_3 (aq., satd.) and extracted with CH_2Cl_2 (3 \times). The combined organics were dried (MgSO_4), filtered, and concentrated to a yellow oil (106 mg), which was purified by silica gel chromatography to provide **7c** as a white solid (77 mg, 0.35 mmol, 41% yield). Compound **7c** was then combined with phenylenediamine (0.038 g, 0.35 mmol) in a vial. The two solids were ground together with a glass rod, and the vial was capped and heated in an oil bath with stirring at 150 $^\circ\text{C}$ for 4 h. The reaction was then cooled to room temperature, and DMF was added. The reaction was subjected to sonication, and the resulting white solid was collected and dried to provide **8c** (8.8 mg, 9% yield).

General Method for LHMDs Cyclization (Method A). LH-MDS (1.65 mL, 1 M in THF, 1.65 mmol, 5.0 equiv) was added dropwise to a solution of ethyl 2-(1H-benzo[d]imidazol-2-yl)acetate (67.6 mg, 0.33 mmol, 1.0 equiv), 2-aminobenzonitrile **6c** (60 mg, 0.5 mmol, 1.5 equiv), and anhydrous THF (15 mL). The resulting solution was stirred at room temperature for 5 h and then quenched with NH_4Cl (aq. sat.). The mixture was diluted with H_2O and extracted with EtOAc (3 \times). The combined organic layers were washed once with water, dried with MgSO_4 , and concentrated to approximately 10 mL. A yellow solid precipitated, which was collected via filtration and dried under reduced pressure to provide **8c** (28 mg). Additional material (16 mg) was obtained by concentrating the filtrate and purifying the resulting solid by silica gel chromatography (5% MeOH/ CH_2Cl_2). Overall 44 mg (48% yield) of **8c** was obtained. ^1H NMR (300 MHz, DMSO- d_6) 11.38 (1 H, s), 8.19 (1 H, d, J = 8.3 Hz), 7.65 (2 H, bs), 7.56 (1 H, dd, J = 8.3, 1.0 Hz), 7.33 (1 H, d, J = 8.3 Hz), 7.23 (1 H, dd, J = 8.3, 1.0 Hz), 7.15 (2 H, m). ^{13}C NMR (75 MHz, DMSO- d_6) 161.6, 155.2, 139.6, 133.4, 128.7, 126.7, 126.2, 125.0, 124.4, 122.5, 116.8, 114.5, 113.3, 89.1. LCMS (m/z) 276.8 (MH^+), R_t 1.68 min. HRMS found m/z 277.1087; $\text{C}_{16}\text{H}_{13}\text{N}_4\text{O}$ requires 277.1083.

Ethyl 2-(6-Methylbenzimidazol-2-yl)acetate (18a).¹⁷ Synthesized as in example **18c**. (80% yield). ^1H NMR (300 MHz, DMSO- d_6) 7.37 (1 H, d, J = 8.1 Hz), 7.27 (1 H, bs), 6.95 (1 H, dd, J = 8.1, 1.5 Hz), 4.11 (2 H, q, J = 7.2 Hz), 3.91 (2 H, s), 3.37 (3 H, s), 1.18 (3 H, t, J = 7.2 Hz). ^{13}C NMR (75 MHz, DMSO- d_6) 168.8, 147.3, 138.0, 136.6, 130.6, 122.9, 114.7, 114.0, 60.7, 35.1, 21.2, 14.0. LCMS (m/z) 219.1 (MH^+), R_t 1.42 min. HPLC R_t 14.90 min. Anal. calcd for $\text{C}_{12}\text{H}_{14}\text{N}_2\text{O}_2$: C 66.04, H 6.47, N 12.48; found C 66.18, H 6.34, N 12.55.

4-Amino-3-(6-methylbenzimidazol-2-yl)hydroquinolin-2-one (19a). Method A (50% yield). ^1H NMR (300 MHz, DMSO- d_6) 11.53 (1 H, s, NH), 8.36 (1 H, d, J = 8.1 Hz), 7.68 (1 H, d, J = 8.7 Hz), 7.62 (1 H, d, J = 8.1 Hz), 7.59 (1 H, bs), 7.41 (1 H, d, J = 7.5 Hz), 7.27 (2 H, m), 2.50 (3 H, s). ^{13}C NMR (75 MHz, DMSO- d_6) 160.9, 154.4, 146.3, 139.0, 134.0, 132.5, 131.0, 125.7, 124.1, 121.6, 116.1, 113.5, 113.3, 112.7, 88.4, 21.2. LCMS (m/z): 291.1 (MH^+), R_t 1.89 min. HPLC R_t 19.66 min. HRMS found m/z 291.1255; $\text{C}_{17}\text{H}_{15}\text{N}_4\text{O}$ requires 291.1240.

Ethyl 2-(5,6-Dimethylbenzimidazol-2-yl)acetate (18b).³⁴ Synthesized as in example **18c** (86% yield). ^1H NMR (300 MHz, DMSO- d_6) 12.0 (1 H, bs, NH), 7.24 (2 H, s), 4.10 (2 H, q, 7.5 Hz), 3.87 (2 H, s), 2.27 (6H, s), 1.17 (3 H, t, J = 7.5 Hz). LCMS (m/z) 233.1 (MH^+), R_t 1.76 min.

4-Amino-3-(5,6-dimethylbenzimidazol-2-yl)hydroquinolin-2-one (19b). Method A (25% yield). ^1H NMR (300 MHz, DMSO- d_6) 11.48 (1H, s, NH), 8.29 (1 H, d, J = 8.1 Hz), 8.20 (1 H, bs, NH), 7.61 (2 H, dd, J = 8.1, 7.5 Hz), 7.54 (2 H, s), 7.35 (1 H, d,

$J = 8.1$ Hz), 7.23 (1 H, dd, $J = 8.1, 7.5$ Hz), 2.38 (6 H, bs). ^{13}C NMR (75 MHz, DMSO- d_6) 161.5, 154.9, 146.2, 139.7, 134.3, 133.2, 131.4, 124.6, 122.3, 116.7, 114.3, 113.3, 89.1, 20.6. LCMS (m/z) 305.3 (MH^+), R_t 2.31 min. HPLC R_t 20.53 min.

5-Morpholin-4-yl-2-nitrophenylamine (21a): General Method for $\text{S}_\text{N}\text{Ar}$ Reaction (Method B). 5-Fluoro-2-nitrophenylamine (30.0 g, 0.19 mol) was dissolved in anhydrous 1-methyl-2-pyrrolidinone (NMP, 40 mL). Triethylamine (58 mL, 0.42 mol, 2.2 equiv) and morpholine (18 mL, 0.21 mol, 1.1 equiv) were added. The reaction vessel was fitted with a reflux condenser and heated at 100 °C for 16 h. The reaction was cooled to room temperature and then poured into 1 L of water. A yellow precipitate formed, which was collected by filtration through a sintered glass funnel, washed with ether, and dried under vacuum to yield **21a** (38.0 g, 91%) as a yellow solid.

Ethyl 2-(5-Morpholin-4-ylbenzimidazol-2-yl)acetate (23a): General Method for Formation of the Benzimidazole Acetate (Method C). A 2 L round-bottom flask was charged with 5-morpholin-4-yl-2-nitrophenylamine (20.0 g, 90 mmol, 1.0 equiv) and anhydrous ethanol (800 mL). Palladium on carbon (10% w/w, 6.6 g) was added, and the reaction vessel was fitted with a 3-way stopcock. The flask was evacuated under vacuum and then filled with hydrogen. The reaction was stirred overnight under a 1 atm of hydrogen gas, with additional hydrogen added as necessary. The reaction was flushed with nitrogen, and ethyl 3-ethoxy-3-imino-propanoate hydrochloride (44.1 g, 220 mmol, 2.4 equiv) was added. The reaction vessel was fitted with a reflux condenser and heated at 90 °C overnight under a positive pressure of nitrogen. The reaction was then cooled to room temperature and filtered through a pad of celite. The filtrate was concentrated under reduced pressure. The resulting residue was dissolved in CH_2Cl_2 (500 mL), neutralized with ammonium hydroxide, and washed with water (2×100 mL). The organic phase was concentrated and filtered through a plug of silica gel using EtOAc. The filtrate was concentrated in vacuo to afford **23a** (21.2 g, 81% yield) as a brown solid (product is very hygroscopic). ^1H NMR (300 MHz, DMSO- d_6) 7.35 (1 H, d, $J = 8.7$ Hz), 6.94 (1 H, d, $J = 1.8$ Hz), 6.89 (1 H, dd, $J = 8.7, 1.8$ Hz), 4.1 (2 H, q, $J = 7.2$ Hz), 3.88 (2 H, s), 3.74 (4 H, m), 3.04 (4 H, m), 1.18 (3 H, t, $J = 7.2$ Hz). ^{13}C NMR (75 MHz, DMSO- d_6) 168.8, 147.4, 146.8, 138.2, 134.3, 115.8, 112.9, 99.9, 66.2, 60.7, 50.4, 35.1, 14.0. LCMS (m/z): 290.1 (MH^+), R_t 1.36 min. HPLC R_t 13.38 min. Anal. calcd for $\text{C}_{15}\text{H}_{19}\text{N}_3\text{O}_3$: C 62.27, H 6.62, N 14.51; found C 62.30, H 6.49, N 14.04.

4-Amino-3-(6-morpholin-4-ylbenzimidazol-2-yl)hydroquinolin-2-one (19c). Method A (61% yield). ^1H NMR (300 MHz, DMSO- d_6) 11.48 (1 H, s), 9.20 (1 H, bs), 8.31 (1 H, d, $J = 8.4$ Hz), 8.11 (1 H, bs), 7.81 (1 H, d, $J = 8.7$ Hz), 7.72 (1 H, d, $J = 8.7$ Hz), 7.59 (1 H, dd, $J = 8.4, 7.2$), 7.38 (1 H, d, $J = 8.4$ Hz), 7.24 (1 H, dd, $J = 8.1, 7.2$), 4.11 (4H, bs), 3.59 (4H, bs). ^{13}C NMR (75 MHz, DMSO- d_6) 162.4, 155.0, 152.6, 139.9, 139.1, 137.0, 133.8, 132.9, 124.6, 122.3, 116.7, 116.2, 115.2, 113.5, 107.5, 90.0, 64.6, 54.7. LCMS (m/z) 362.1 (MH^+), R_t 1.65 min. HPLC R_t 18.16 min; Anal. calcd for $\text{C}_{20}\text{H}_{19}\text{N}_5\text{O}_2 + 0.6 \text{ H}_2\text{O}$: C 64.33, H 5.49, N 18.76; found C 64.21, H 5.37, N 18.37.

5-(4-Methylpiperazinyl)-2-nitrophenylamine (21b).³⁵ Method B (96% yield). ^1H NMR (300 MHz, DMSO- d_6) 7.78 (1 H, dd, $J = 9.6, 0.9$ Hz), 7.24 (2 H, bs), 6.34 (1 H, dd, $J = 9.6, 2.2$ Hz), 6.19 (1 H, d, $J = 2.2$ Hz), 3.27 (4 H, t, $J = 4.8$ Hz), 2.36 (4H, t, $J = 4.8$ Hz), 2.17 (3 H, s). ^{13}C NMR (75 MHz, DMSO- d_6) 155.0 (C), 148.3 (C), 127.1 (CH), 122.9 (C), 105.4 (CH), 97.5 (CH), 54.1 (CH₂), 46.1 (CH₂), 45.6 (CH₃). LCMS m/z 237.3 (MH^+), R_t 1.23 min. Anal. calcd for $\text{C}_{11}\text{H}_{16}\text{N}_4\text{O}_2$: C, 55.92; H, 6.83; N, 23.71. Found: C, 55.96; H, 6.62, N, 23.68.

Ethyl 2-[6-(4-Methylpiperazinyl)benzimidazol-2-yl]acetate (23b). Method C (83% yield). ^1H NMR (300 MHz, DMSO- d_6) 7.33 (1 H, d, $J = 8.7$ Hz), 6.92 (1 H, bs), 6.87 (1 H, d, $J = 8.7$ Hz), 4.10 (2 H, q, $J = 7.2$ Hz), 3.87 (2 H, s), 3.06 (4 H, m), 2.45 (4 H, m), 2.20 (3 H, s), 1.18 (3 H, t, $J = 7.2$ Hz). ^{13}C NMR (75 MHz, DMSO- d_6) 168.9, 147.5, 146.6, 136.2, 136.0, 118.5, 113.3, 98.1, 60.7, 54.9, 50.06, 45.7, 35.1, 14.0. LCMS (m/z) 303.1 (MH^+), R_t 1.15 min. HPLC R_t 9.85 min.

4-Amino-3-[6-(4-methylpiperazinyl)benzimidazol-2-yl]hydroquinolin-2-one (19d). Method A (60% yield). ^1H NMR (300 MHz, DMSO- d_6) 11.47 (1 H, s, NH), 11.32 (1 H, bs, NH), 8.26 (1 H, d, $J = 8.1$ Hz), 7.63 (2 H, dd, $J = 8.4, 8.1$ Hz), 7.35 (1 H, d, $J = 8.4$ Hz), 7.27 (2 H, bs), 7.23 (1 H, d, $J = 8.1$ Hz), 3.82 (2 H, m), 3.53 (2 H, m), 3.24 (4 H, m), 2.82 (3 H, s). ^{13}C NMR (75 MHz, DMSO- d_6) 161.2, 154.0, 147.3, 146.9, 138.7, 134.1, 132.3, 128.4, 123.9, 121.6, 116.0, 115.5, 114.6, 112.8, 100.5, 109.0, 52.1, 47.0, 41.9. LCMS (m/z) 375.2 (MH^+), R_t 1.38 min. HPLC R_t 14.09 min. HRMS found m/z 375.1895; $\text{C}_{21}\text{H}_{23}\text{N}_6\text{O}$ requires 375.1927. Anal. calcd for $\text{C}_{21}\text{H}_{22}\text{N}_6\text{O}$: C 67.36, H 5.92, N 22.44; found C 67.15, H 5.84, N 22.27.

5-(4-Methyl(1,4-diazaperhydroepinyl))-2-nitrophenylamine (21c). Method B (20% yield). ^1H NMR (300 MHz, DMSO- d_6) 7.81 (1 H, d, $J = 9.9$ Hz), 7.23 (2 H, bs, NH₂), 6.25 (1 H, dd, $J = 9.9, 2.7$ Hz), 6.05 (1 H, d, $J = 2.7$ Hz), 3.56 (2 H, m), 3.49 (2 H, m), 3.62 (2 H, m), 2.48 (2 H, m), 2.28 (3 H, s), 1.88 (2 H, m). ^{13}C NMR (75 MHz, DMSO- d_6) 153.7, 148.4, 127.5, 122.1, 104.0, 94.6, 56.7, 55.9, 48.1, 47.9, 45.7, 26.4. LCMS (m/z) 251.3 (MH^+), R_t 1.57 min. Anal. calcd for $\text{C}_{12}\text{H}_{18}\text{N}_4\text{O}_2$: C 57.58, H 7.25, N 22.38; found C 57.03, H 7.11, N 22.31.

Ethyl 2-[6-(4-Methyl-1,4-diazaperhydroepinyl)benzimidazol-2-yl]acetate (23c). Method C (53% yield). ^1H NMR (300 MHz, DMSO- d_6) 7.26 (1 H, m), 6.62 (2 H, m), 4.09 (2 H, q, $J = 7.2$ Hz), 3.83 (2 H, s), 3.50 (2 H, m), 3.41 (2 H, m), 2.62 (2 H, m), 2.44 (2 H, m), 2.25 (3 H, s), 1.90 (2 H, m), 1.18 (3 H, t, $J = 7.2$ Hz). LCMS (m/z) 317.4 (MH^+), R_t 1.47 min.

4-Amino-3-[6-(4-methyl(1,4-diazaperhydroepinyl))benzimidazol-2-yl]hydroquinolin-2-one (19e). Method A (5% yield). ^1H NMR (300 MHz, DMSO- d_6) 11.67 (1 H, bs, NH), 11.48 (1 H, s, NH), 8.31 (1 H, d, $J = 8.1$ Hz), 7.64 (1 H, d, $J = 9.3$ Hz), 7.58 (1 H, dd, $J = 8.4, 7.2$ Hz), 7.36 (1 H, d, $J = 8.4$ Hz), 7.27 (2 H, bs), 7.20 (1 H, dd, $J = 8.1, 7.2$ Hz), 3.96 (2 H, m), 3.60 (3 H, m), 3.44 (2 H, m), 3.23 (1 H, m), 2.78 (3 H, s), 2.41 (1 H, m), 2.30 (1 H, m). ^{13}C NMR (75 MHz, DMSO- d_6) 161.7, 154.9, 146.8, 145.5, 139.6, 134.7, 133.2, 127.0, 124.8, 122.3, 116.7, 115.0, 113.7, 113.4, 98.3, 89.2, 55.3, 50.7, 47.1, 43.7, 23.5. LCMS (m/z) 389.4 (MH^+), R_t 1.72 min.

(3S)-1-(3-Amino-4-nitrophenyl)pyrrolidin-3-yl]dimethylamine (21d). Method B (88% yield); mp 148–149 °C. ^1H NMR (300 MHz, acetone- d_6) 7.90 (1 H, d, $J = 9.5$ Hz), 6.88 (2 H, bs, NH₂), 6.09 (1 H, dd, $J = 9.5, 2.7$), 5.90 (1H, d, $J = 2.7$ Hz), 3.56 (2 H, m), 3.36 (1 H, m), 3.15 (1 H, app. t, $J = 8.4$ Hz), 2.81 (1 H, m), 2.24 (6 H, s), 2.22 (1 H, m), 1.88 (1 H, m). ^{13}C NMR (75 MHz, DMSO- d_6) 151.8, 148.3, 127.5, 122.4, 104.3, 94.5, 64.5, 51.7, 46.6, 40.3, 29.3. LCMS (m/z): 251.2 (MH^+), R_t 1.34 min. HPLC: R_t 13.48 min; $[\alpha]_D^{22} = -16.3$ ($c = 0.57$, DMSO).

Ethyl 2-[5-[(3S)-3-(dimethylamino)pyrrolidinyl]benzimidazol-2-yl]acetate (23d). Method C (76% yield); mp 135 °C (decomposition). ^1H NMR (300 MHz, DMSO- d_6) 7.30 (1 H, d, $J = 9.3$ Hz), 6.50 (1 H, s), 6.41 (1 H, d, $J = 9.3$ Hz), 4.12 (2 H, q, $J = 7.2$ Hz), 3.85 (2 H, s), 3.41 (1 H, m), 3.29 (2 H, m), 3.04 (1 H, m), 2.80 (1 H, m), 2.21 (6 H, s), 2.15 (1 H, m), 1.82 (1 H, m), 1.20 (3 H, t, $J = 7.2$ Hz). LCMS m/z 317.1 (MH^+), R_t 1.45 min. HPLC R_t 11.6 min; $[\alpha]_D^{22} = -25.3$ ($c = 1$, DMSO).

3-[5-[(3S)-3-(Dimethylamino)pyrrolidinyl]benzimidazol-2-yl]-4-aminohydroquinolin-2-one (19f). Method A (1.5 g, 43% yield); mp 280 °C (decomposition). ^1H NMR (300 MHz, DMSO- d_6) 11.79 (1 H, bs, NH), 11.46 (1 H, s, NH), 8.27 (1 H, d, $J = 7.8$ Hz), 8.1 (1 H, bs, NH), 7.61 (1 H, d, $J = 9.0$ Hz), 7.60 (1 H, app. t, $J = 5.4$ Hz), 7.34 (1 H, d, $J = 7.8$ Hz), 7.23 (1 H, app. t, $J = 7.8$ Hz), 6.88 (1 H, d, $J = 9.0$ Hz), 6.80 (1 H, s), 4.04 (1 H, m), 3.70 (2 H, m), 3.57 (1 H, m), 3.35 (1 H, m), 2.81 (6 H, s), 2.44 (2 H, m). ^{13}C NMR (75 MHz, DMSO- d_6) 160.83, 154.02, 144.97, 138.95, 132.44, 123.94, 121.64, 116.03, 114.39, 112.69, 111.61, 94.37, 88.66, 63.82, 49.43, 47.02, 41.26, 40.70, 26.51. LCMS m/z 389.1 (MH^+), R_t 1.72 min. HRMS found m/z 389.2050; $\text{C}_{22}\text{H}_{25}\text{N}_6\text{O}$ requires 389.2084; $[\alpha]_D^{22} = -21.5$ ($c = 0.5$, DMSO). Anal. calcd for $\text{C}_{22}\text{H}_{24}\text{N}_6\text{O} + 0.5\text{H}_2\text{O}$: C 66.48, H 6.34, N 21.14; found C 66.15, H 6.01, N 21.05.

5-(2-Morpholin-4-ylethoxy)-2-nitrophenylamine (24). Diisopropyl azodicarboxylate (14 mL, 71.4 mmol) was added dropwise

to a stirred solution of 3-amino-4-nitrophenol (10.1 g, 64.9 mmol), triphenylphosphine (18.7 g, 71.4 mmol), and *N*-(2-hydroxyethyl)-morpholine (7.9 mL, 64.9 mmol) in THF (100 mL) at 0 °C. The mixture was allowed to warm to room temperature and left to stir for 18 h. The solvent was then evaporated, and the product was purified by flash chromatography (98:2 CH₂Cl₂:MeOH), yielding **24** as a dark reddish-brown syrup (5.62 g, 32%). LCMS (*m/z*) 268.0 (MH⁺), *R*_t 1.01 min.

4-(2-Morpholin-4-ylethoxy)benzene-1,2-diamine (25). To a solution of 5-(2-morpholin-4-ylethoxy)-2-nitrophenylamine (5.62 g) in EtOH (100 mL), Pd/C (200 mg) was added. The reaction vessel was purged (3×) with nitrogen and then stirred under a H₂ atmosphere for 18 h. The reaction was filtered through a celite plug, and the plug was washed with EtOH. The solution was used immediately in the next step. LC/MS (*m/z*) 238.3 (MH⁺) *R*_t 0.295 min.

Ethyl 2-[5-(2-Morpholin-4-ylethoxy)benzimidazol-2-yl]acetate (26). To the solution of **25** in EtOH described above (125 mL), ethyl 3-ethoxy-3-iminopropanoate hydrochloride (4.06 g, 20.8 mmol) was added. This reaction mixture was heated for 18 h at 70 °C, at which time the solvent was evaporated and the residue was taken up in CH₂Cl₂. The organic layer was washed once with H₂O and then purified by flash chromatography (10:1:2 CH₂Cl₂:MeOH:EtOAc) to yield **26** as a dark reddish-brown syrup (4.94 g, 70% yield over two steps). ¹H NMR (300 MHz, CDCl₃) 7.4 (1 H, broad s), 6.9 (1 H, broad s), 6.83 (1 H, dd, *J* = 9.0 Hz), 4.18 (2 H, q), 4.1 (2 H, t, *J* = 5.4 Hz), 3.96 (2 H, s), 3.71 (4 H, t, *J* = 5.1 Hz), 2.77 (2 H, t, *J* = 5.7 Hz), 2.54 (4 H, t, *J* = 4.8 Hz), 1.25 (3 H, t, *J* = 7.2 Hz). LCMS (*m/z*) 334.4 (MH⁺) *R*_t 1.08 min.

4-Amino-3-[5-(2-morpholin-4-ylethoxy)-benzimidazol-2-yl]hydroquinolin-2-one (19g). Method A (239 mg, 14% yield). ¹H NMR (300 MHz, D₂O) 7.83 (d, *J* = 8.7, 1H), 7.59 (t, *J* = 7.2, 1H), 7.52 (d, *J* = 8.7, 1H), 7.24 (t, *J* = 6.9, 1H), 7.19 (d, *J* = 7.8, 1H), 7.10 (s, 1H), 6.98 (dd, *J* = 9, 1H), 4.32 (t, *J* = 5.1, 2H), 4.11 (2H, broad m), 3.88 (broad m, 2H), 3.64 (t, *J* = 5.1, 2H), 3.60 (broad m, 2H), 3.33 (broad m, 2H). Note: At 50 °C, the broad multiplets at 3.33, 3.60, 3.88, and 4.11 resolved into two broad multiplets of 4 H each (δ 3.73, 4.28). LCMS (*m/z*) 406.4 (MH⁺) *R*_t 1.56 min. HRMS found *m/z* 406.1850; C₂₂H₂₄N₅O₃ requires 406.1873.

2-[5-(Methoxycarbonyl)benzimidazol-2-yl]acetate (18c). Methyl 3,4-diaminobenzoate (14.85 g, 89.4 mmol, 1 equiv) was stirred with ethyl 3-ethoxy-3-iminopropanoate hydrochloride (26.3 g, 134.9 mmol, 1.5 equiv) in EtOH (300 mL) at 70 °C overnight. The reaction mixture was cooled to room temperature, and the excess unreacted ethyl 3-ethoxy-3-iminopropanoate hydrochloride was removed by filtration. The EtOH was removed under reduced pressure, and the residue was dissolved in water and extracted with CH₂Cl₂ (3×). The organic extracts were dried over Na₂SO₄, and the solvent removed under reduced pressure. The solid was triturated with Et₂O to yield **18c** as an off-white solid (18.4 g, 78%). ¹H NMR (300 MHz, DMSO-*d*₆) 8.15 (1 H, d, *J* = 1.5 Hz), 7.81 (1 H, dd, *J* = 8.4, 1.5 Hz), 7.61 (1 H, d, *J* = 8.4 Hz), 4.14 (2 H, q, *J* = 7.2 Hz), 4.04 (2 H, s), 3.86 (3 H, s), 1.20 (3 H, t, *J* = 7.2). ¹³C NMR (75 MHz, DMSO-*d*₆) 169.2, 167.5, 151.3, 143.1, 139.3, 123.7, 123.5, 117.7, 115.3, 61.6, 52.6, 35.8, 14.7. LCMS (*m/z*) 263.3 (MH⁺), *R*_t 1.82 min. Anal. calcd for C₁₃H₁₄N₂O₄: C 59.41, H 5.12, N 10.51; found C 59.54, H 5.38, N 10.68.

Methyl 2-(4-Amino-2-oxo-3-hydroquinolyl) benzimidazole-6-carboxylate (19ad). Method A (21% yield). ¹H NMR (300 MHz, DMSO-*d*₆) 13.28 (1 H, s), 11.42 (1 H, s), 8.37 (1 H, bs), 8.24 (1 H, d, *J* = 6.3 Hz), 8.20 (1 H, d, *J* = 4.6 Hz), 7.80 (1 H, d, *J* = 8.0 Hz), 7.74 (1 H, dd, *J* = 8.0, 4.6 Hz), 7.56 (1 H, dd, *J* = 8.0, 1.0 Hz), 7.34 (1 H, d, *J* = 8.0 Hz), 7.24 (1 H, dd, *J* = 8.0, 1.0 Hz), 3.85 (3 H, s).

2-(4-Amino-2-oxo-3-hydroquinolyl)benzimidazole-6-carboxylic acid (19ae). The crude material obtained in the previous step was dissolved in a 1:1 mixture of EtOH and 30% aq KOH (10 mL) and stirred overnight at 70 °C. The reaction mixture was cooled and acidified with 1N HCl. A precipitate formed. The solid was filtered, washed with water, and dried to obtain **19ae** (190 mg, 40%) as a brown solid. ¹H NMR (300 MHz, DMSO-*d*₆) 11.46 (1 H, s,

NH), 9.40 (1 H, bs, NH), 8.30 (1 H, d, *J* = 1.5 Hz), 8.28 (1 H, d, *J* = 8.1 Hz), 7.88 (1 H, dd, *J* = 8.7, 1.5 Hz), 7.76 (1 H, d, *J* = 8.7 Hz), 7.60 (1 H, dd, *J* = 8.1, 7.5 Hz), 7.37 (1 H, d, *J* = 8.4 Hz), 7.25 (1 H, dd, *J* = 8.4, 7.5 Hz). ¹³C NMR (75 MHz, DMSO-*d*₆) 168.4, 162.5, 155.1, 153.4, 139.5, 139.1, 135.5, 132.9, 125.5, 124.5, 122.3, 116.7, 114.7, 113.5, 90.1. LCMS (*m/z*) 321.3 (MH⁺), *R*_t 2.25 min.

4-Amino-3-{6-[(4-methylpiperazinyl)carbonyl]benzimidazol-2-yl}hydroquinolin-2-one (19h). A mixture of **19ae** (70 mg, 0.22 mmol, 1.0 equiv), 1-methyl piperazine (0.024 mL, 0.22 mmol, 1.0 equiv), 1-(3-dimethylaminopropyl)-3-ethylcarbodiimide hydrochloride (EDC 50 mg, 0.26 mmol, 1.2 equiv), 1-hydroxy-7-azabenzotriazole (HOAT, 35 mg, 0.26 mmol, 1.2 equiv), and Et₃N (0.06 mL, 0.44 mmol, 2.5 equiv) in DMF (3 mL) was stirred at 23 °C for 20 h. The reaction mixture was partitioned between H₂O and EtOAc. The combined organic layers were dried with Na₂SO₄ and concentrated. Water was added, and the precipitate was filtered and dried. The crude solid was purified by reverse phase HPLC to afford **19h** (29.8 mg, 34%). ¹H NMR (300 MHz, DMSO-*d*₆) 8.20 (1 H, d, *J* = 8.1 Hz), 7.81 (1 H, d, *J* = 1.5 Hz), 7.77 (1 H, d, *J* = 8.4 Hz), 7.59 (1 H, dd, *J* = 8.1, 7.2 Hz), 7.42 (1 H, dd, *J* = 8.4, 1.2 Hz), 7.33 (1 H, d, *J* = 8.4 Hz), 7.23 (1 H, dd, *J* = 8.4, 7.2 Hz), 4.12 (2 H, m), 3.40 (4 H, m), 3.11 (2 H, m). ¹³C NMR (75 MHz, DMSO-*d*₆) 169.6, 161.6, 154.4, 151.2, 138.5, 135.7, 134.3, 132.3, 129.1, 124.0, 122.3, 121.6, 116.0, 114.2, 113.6, 112.8, 89.1, 51.9, 42.0, 40.1. LCMS (*m/z*) 403.3 (MH⁺), *R*_t 1.80 min. Anal. calcd for C₂₂H₂₂N₆O₂ + 2H₂O: C 60.26, H 5.98, N 19.17; found C 60.38, H 5.48, N 18.84.

4-amino-3-(6-(hydroxymethyl)-1H-benzof[*d*]imidazol-2-yl)quinolin-2(1H)-one (19af). A suspension of methyl 2-(4-amino-2-oxo-3-hydroquinolyl) benzimidazole-6-carboxylate **19ad** (1.0 g, 3.1 mmol, 1.0 equiv) in toluene (100 mL) was treated with DIBAL-H (10.3 mL of 1.5 M soln in toluene, 15.5 mmol, 5.0 equiv) at room temperature. The reaction mixture was stirred for 10 h and was then treated with NaF (2.6 g, 62 mmol, 20 equiv) followed by water (0.27 mL, 15 mmol, 4.8 equiv). The reaction was stirred at room temperature for an additional 1.5 h, and then DMF was added. The resulting mixture was heated at 100 °C for 1 h and then filtered. The filtrate was evaporated to one-quarter of the original volume and treated with 50 mL of water. The resulting solid was collected and dried to give **19af** (475 mg, 50% yield). ¹H NMR (300 MHz, DMSO-*d*₆) 13.28 (1 H, s), 11.42 (1 H, s), 8.19 (1 H, d, *J* = 8.8 Hz), 7.58 (3 H, m), 7.34 (1 H, d, *J* = 8.8 Hz), 7.26 (2 H, m), 4.58 (2 H, s), 4.5–4.9 (1 H, bs). LCMS (*m/z*) 307.1 (MH⁺), *R*_t 1.47 min.

2-(4-Amino-2-oxo-1,2-dihydroquinolin-3-yl)-1H-benzof[*d*]imidazole-6-carbaldehyde (19ag). **19af** (320 mg, 1.04 mmol, 1.0 equiv) was dissolved in DMA (4 mL), and MnO₂ (450 mg, 5.2 mmol, 5.0 equiv) was added. The reaction mixture was heated under microwave irradiation at 140 °C for 10 min. The reaction mixture was then filtered through celite, and water was added to the filtrate. The resulting solid was collected and dried to give **19ag** (310 mg, 97% yield). ¹H NMR (300 MHz, DMSO-*d*₆) 13.28 (1 H, s), 11.42 (1 H, s), 10.00 (1 H, s), 8.42 (1 H, bs), 8.24 (1 H, d, *J* = 6.3 Hz), 8.19 (1 H, d, *J* = 4.6 Hz), 7.86 (1 H, d, *J* = 8.0 Hz), 7.74 (1 H, dd, *J* = 8.0, 4.6 Hz), 7.58 (1 H, dd, *J* = 8.0, 1.0 Hz), 7.34 (1 H, d, *J* = 8.0 Hz), 7.23 (1 H, dd, *J* = 8.0, 1.0 Hz). LCMS (*m/z*) 305.1 (MH⁺), *R*_t 2.47 min.

4-Amino-3-(6-((4-methylpiperazin-1-yl)methyl)-1H-benzof[*d*]imidazol-2-yl)quinolin-2(1H)-one (19i). **19ag** (250 mg, 0.82 mmol, 1.0 equiv) was suspended in MeOH (5 mL). Piperazine (123 mg, 1.23 mmol, 1.5 equiv) and HOAc (0.15 mL, 2.46 mmol, 3.0 equiv) were added followed by NaBH₃CN (257 mg, 4.1 mmol, 5.0 equiv). The reaction was heated at 90 °C for 6 h in a glass bomb. The solution was cooled and then poured into water and extracted with EtOAc. The organic layer was dried and concentrated, and the resulting oil was purified by reverse phase HPLC. The purified fractions were combined, neutralized with NaHCO₃ (aq, sat.), and extracted with EtOAc (2×). The organic extracts were combined, dried, and concentrated to give **19i** (160 mg, 50% yield). LCMS (*m/z*) 389.1 (MH⁺), *R*_t 1.46 min.

4-Amino-3-(6-(methylamino)-1H-benzo[d]imidazol-2-yl)quinolin-2(1H)-one (19ah). Method A (63% yield). HRMS found m/z 306.1354; $C_{17}H_{15}N_5O$ requires 306.1349.

N-(2-(4-Amino-2-oxo-1,2-dihydroquinolin-3-yl)-1H-benzo[d]imidazol-6-yl)-2-(dimethylamino)-N-methylacetamide (19j). To a solution of **19ah** (75 mg, 0.25 mmol, 1.0 equiv) in DMA (6 mL) was added 2-(dimethylamino)acetic acid (38 mg, 0.37 mmol, 1.5 equiv), EDC (57.4, 0.37 mmol, 1.5 equiv), HOBt (50 mg, 0.37 mmol, 1.5 equiv), and Et_3N (0.104 mL, 0.74 mmol, 3 equiv). The reaction mixture was stirred at room temperature for 12 h. The reaction mixture was then concentrated to a thick oil and triturated with water. The resulting solid was collected and purified by reverse phase HPLC. The purified fractions were combined, neutralized with $NaHCO_3$ (aq, sat.), and extracted with $EtOAc$ (2 \times). The organic extracts were combined, dried, and concentrated to provide **19j** (70 mg, 72% yield). LCMS (m/z) 391.2 (MH^+), R_t 1.68 min.

4-Amino-5-fluoro-3-(6-(4-methylpiperazin-1-yl)-1H-benzo[d]imidazol-2-yl)quinolin-2(1H)-one (5). Method A (60% yield). 1H NMR (300 MHz, $DMSO-d_6$) 11.66 (1H, s, NH), 9.73 (1H, bs, NH), 7.66 (1H, d, $J = 9.1$ Hz), 7.59 (1H, ddd, $J = 8.5, 8.0, 6.0$ Hz), 7.29 (1H, dd, $J = 9.1, 1.5$ Hz), 7.23 (1H, s), 7.15 (1H, d, $J = 8.0$ Hz), 7.04 (1H, dd, $J = 13.8, 8.5$ Hz), 3.86 (2H, d, $J = 12.7$ Hz), 3.56 (2H, d, $J = 11.4$ Hz), 3.23 (2H, m), 3.07 (2H, m), 2.88 (3H, s). ^{13}C NMR (75 MHz, $DMSO-d_6$) 162.5, 159.2, 151.9 (d, $J = 42.3$ Hz), 147.0, 140.2, 136.5, 133.2, 132.9 (d, $J = 14.1$ Hz), 118.1, 114.7, 113.9, 113.0, 108.6 (d, $J = 18.9$ Hz), 104.9, 103.3, 99.4, 91.5, 48.4, 43.6. Anal. calcd for $C_{21}H_{21}N_6OF \cdot 1.5H_2O$: C 60.13, H 5.77, N 20.04, F 4.53; found C 60.74, H 5.98, N 18.50, F 4.13. HRMS found m/z 393.1812; $C_{21}H_{22}N_6OF$ requires 393.1833.

4-Amino-5-chloro-3-[6-(4-methylpiperazinyl)benzimidazol-2-yl]hydroquinolin-2-one (19k). Method A (8% yield). ^{13}C NMR (75 MHz, $DMSO-d_6$) 161.2, 154.0, 147.3, 146.9, 138.7, 134.1, 132.3, 127.4, 123.9, 120.4, 116.6, 115.5, 114.6, 100.5, 89.0, 52.1, 47.0, 41.9. HRMS found m/z 409.1550; $C_{21}H_{22}N_6OCl$ requires 409.1538.

4-Amino-5-methyl-3-[6-(4-methylpiperazinyl)benzimidazol-2-yl]hydroquinolin-2-one (19l). Method A (8% yield). 1H NMR (300 MHz, $DMSO-d_6$) 11.56 (1H, bs, NH), 11.37 (1H, s, NH), 7.62 (1H, d, $J = 9.0$ Hz), 7.41 (1H, dd, $J = 8.4, 7.5$ Hz), 7.26 (1H, d, $J = 2.1$ Hz), 7.21 (1H, d, $J = 8.4$ Hz), 7.20 (1H, dd, $J = 9.0, 2.1$ Hz), 7.00 (1H, d, $J = 7.5$ Hz), 3.78 (2H, m), 3.51 (2H, m), 3.25 (4H, m), 2.85 (3H, s), 2.80 (3H, s). ^{13}C NMR (75 MHz, $DMSO-d_6$) 160.6, 157.1, 147.6, 146.9, 139.9, 136.0, 133.7, 131.5, 127.9, 125.8, 115.6, 114.4, 112.8, 100.3, 89.4, 52.0, 47.0, 41.9, 23.2. LCMS (m/z) 389.5 (MH^+), R_t 1.88 min. HPLC R_t 15.03 min. HRMS found m/z 389.2053; $C_{22}H_{25}N_6O$ requires 389.2084; Anal. calcd for $C_{22}H_{24}N_6O + 0.5H_2O$: C 66.64, H 6.71, N 20.73; found C 66.36, H 6.14, N 20.00.

4-Amino-5-(methylamino)-3-(6-(4-methylpiperazin-1-yl)-1H-benzo[d]imidazol-2-yl)quinolin-2(1H)-one (19m). Compound **5** (50 mg, 0.13 mmol, 1.0 equiv) was dissolved in a solution of $MeNH_2$ (6 M in $EtOH$, 3 mL, 18 mmol, 140 equiv) and heated at 180 °C in a sealed vessel for 48 h. The reaction mixture was cooled, concentrated, and purified via reverse phase HPLC to provide **19m** (21 mg, 41% yield) as a yellow solid. 1H NMR (300 MHz, $DMSO-d_6$) 11.12 (1H, s), 9.8 (1H, bs), 9.75 (1H, bs), 7.51 (1H, d, $J = 8.7$ Hz), 7.35 (1H, t, $J = 8.1$ Hz), 7.24 (1H, bs), 6.94 (1H, dd, $J = 8.1, 2.4$ Hz), 6.78 (1H, d, $J = 8.1$ Hz), 6.57 (1H, d, $J = 7.8$ Hz), 3.75 (1H, m), 3.55 (1H, m), 3.24 (1H, m), 3.0 (1H, m), 2.9 (3H, s), 2.71 (3H, s).

4-Amino-6-fluoro-3-[6-(4-methylpiperazinyl)benzimidazol-2-yl]hydroquinolin-2-one (19n). Method A (25% yield). 1H NMR (300 MHz, $DMSO-d_6$) 11.51 (1H, s, NH), 11.30 (1H, bs, NH), 8.17 (1H, dd, $J_{H-F} = 10.5, J_{H-H} = 2.1$ Hz), 7.62 (1H, d, $J = 9.0$ Hz), 7.58 (1H, dd, $J_{H-F} = 11.1, J_{H-H} = 8.7$ Hz), 7.37 (1H, dd, $J_{H-H} = 8.7, J_{H-F} = 7.4$ Hz), 7.26 (1H, bs), 7.20 (1H, bd, $J = 9.0$ Hz), 3.78 (2H, m), 3.50 (2H, m), 3.20 (4H, m), 2.81 (3H, s). ^{13}C NMR (75 MHz, $DMSO-d_6$) 161.6, 157.8 (d, $J_{C-F} = 236$ Hz, C *ipso*), 154.2, 147.8, 147.3, 136.4, 134.4, 128.5, 121.3 (d, $J_{C-F} = 24.5$ Hz), 118.8, 116.7, 115.3, 114.2 (d, $J_{C-F} = 8.0$ Hz), 110.2 (d, $J_{C-F} = 27.0$ Hz), 101.1, 90.1 52.7, 47.7, 42.7, 23.5. LCMS (m/z)

393.3 (MH^+), R_t 1.84 min. HRMS found m/z 393.1846; $C_{21}H_{22}N_6OF$ requires 393.1833. Anal. calcd for $C_{21}H_{21}FN_6O$: C 64.24, H 5.39, N 21.42; found C 64.87, H 5.24, N 20.91.

4-Amino-6-chloro-3-[6-(4-methylpiperazinyl)benzimidazol-2-yl]hydroquinolin-2-one (19o). Method A (46% yield). 1H NMR (300 MHz, $DMSO-d_6$) 11.5 (1H, s), 9.6 (1H, bs), 8.33 (1H, d, $J = 2.1$ Hz), 7.60 (2H, dd, $J = 8.7, 2.1$ Hz), 7.34 (1H, d, $J = 8.7$ Hz), 7.28 (1H, s), 6.97 (1H, dd, $J = 9.0, 2.1$ Hz), 3.75 (1H, m), 3.55 (1H, m), 3.24 (1H, m), 3.0 (1H, m), 2.9 (3H, s). ^{13}C NMR (75 MHz, $DMSO-d_6$) 161.5, 153.8, 147.6, 147.3, 138.4, 134.4, 132.9, 126.6, 124.0, 118.7, 116.6, 115.2, 114.6, 101.1, 89.9, 52.6, 47.6, 42.7. HRMS found m/z 409.1550; $C_{21}H_{22}N_6OCl$ requires 409.1538.

4,6-Diamino-3-(6-(4-methylpiperazin-1-yl)-1H-benzo[d]imidazol-2-yl)quinolin-2(1H)-one (19p). Method A (45% yield). 1H NMR (300 MHz, $DMSO-d_6$) 11.35 (1H, s), 9.91 (1H, bs), 7.71 (1H, s), 7.55 (1H, d, $J = 8.8$ Hz), 7.29 (3H, m), 6.96 (1H, dd, $J = 8.8, 1.8$ Hz), 3.75 (1H, m), 3.55 (1H, m), 3.24 (1H, m), 3.0 (1H, m), 2.9 (3H, s). ^{13}C NMR (75 MHz, $DMSO-d_6$) 162.6, 159.3, 158.8, 153.1, 151.8, 146.6, 136.1, 130.5, 125.9, 119.1, 117.8, 115.7, 115.2, 114.7, 114.3, 91.7, 53.2, 48.1, 42.8.

4-Amino-6-(dimethylamino)-3-[6-(4-methylpiperazinyl)benzimidazol-2-yl]hydroquinolin-2-one (19q). Method A (48% yield). 1H NMR (300 MHz, $DMSO-d_6$) 11.17 (1H, s), 9.90 (1H, bs), 7.58 (1H, d, $J = 8.7$ Hz), 7.42 (1H, s), 7.25 (3H, m), 7.0 (1H, dd, $J = 9.0, 2.4$ Hz), 3.75 (1H, m), 3.55 (1H, m), 3.24 (1H, m), 3.0 (1H, m), 2.9 (3H, s). ^{13}C NMR (75 MHz, $DMSO-d_6$) 162.1, 159.6, 159.1, 153.8, 151.4, 146.9, 144.9, 132.4, 122.7, 121.4, 118.8, 117.5, 115.5, 115.0, 114.1, 111.0, 107.9, 101.9, 90.9, 53.2, 48.0, 42.8. HRMS found m/z 418.2360; $C_{23}H_{28}N_7O$ requires 418.2349.

N-(4-Amino-3-(6-(4-methylpiperazin-1-yl)-1H-benzo[d]imidazol-2-yl)-2-oxo-1,2-dihydroquinolin-6-yl)benzamide (19r). To a solution of **19p** (20 mg, 0.05 mmol, 1.0 equiv) in 1.0 mL of N,N -dimethylacetamide (1.0 mL) was added benzoyl chloride (14 mg, 0.10 mmol, 2.0 equiv) followed by Et_3N (0.23 mL, 1.65 mmol, 5 equiv). The resulting solution was stirred at room temperature for 8 h. The reaction was concentrated and purified by reverse phase HPLC to provide **19r** (21 mg, 79% yield) as a yellow solid. 1H NMR (300 MHz, $DMSO-d_6$) 11.4 (1H, s), 10.4 (1H, s), 9.85 (1H, bs), 8.5 (1H, s), 8.0 (2H, m), 7.73 (2H, dd, $J = 2.4, 9.3$ Hz), 7.54 (4H, m), 7.33 (1H, d, $J = 8.7$ Hz), 7.27 (1H, d, $J = 1.8$ Hz), 7.01 (1H, dd, $J = 2.1, 8.7$ Hz), 3.75 (1H, m), 3.55 (1H, m), 3.24 (1H, m), 3.0 (1H, m), 2.9 (3H, s). HRMS found m/z 494.2330; $C_{28}H_{28}N_7O_2$ requires 494.2298.

4-Amino-6-(benzylamino)-3-(6-(4-methylpiperazin-1-yl)-1H-benzo[d]imidazol-2-yl)quinolin-2(1H)-one (19s). To a solution of **19p** (20 mg, 0.05 mmol, 1.0 equiv) in 1.0 mL of $MeOH/CH_2Cl_2/$ $AcOH$ (2:2:1) was added benzaldehyde (11 mg, 0.10 mmol, 2.0 equiv) followed by BH_3/Pyr (0.3 mL of ~ 8 M). The resulting solution was stirred at room temperature for 8 h. The reaction mixture was quenched with H_2O , and the solid was purified by reverse phase HPLC to provide **19s** (19 mg, 82% yield) as a yellow solid. 1H NMR (300 MHz, $DMSO-d_6$) 11.09 (1H, s), 9.9 (1H, bs), 7.75 (1H, d, $J = 8.6$ Hz), 7.44 (2H, m), 7.33 (2H, m), 7.25 (3H, m), 7.04 (3H, m), 4.40 (2H, s), 3.75 (1H, m), 3.55 (1H, m), 3.24 (1H, m), 3.0 (1H, m), 2.9 (3H, s). ^{13}C NMR (75 MHz, $DMSO-d_6$) 161.9, 159.2, 158.8, 153.7, 146.7, 143.9, 140.1, 130.9, 128.9, 128.5, 127.6, 122.0, 117.5, 114.7, 114.2, 103.2, 90.8, 53.2, 48.1, 48.0, 42.8.

4-Aminobenzene-1,3-dicarbonitrile (27d).³⁶ A dry round-bottom flask was charged with 2-amino-5-bromo benzonitrile (1.5 g, 7.5 mmol, 1.0 equiv) and zinc cyanide (880 mg, 7.5 mmol, 1.0 equiv) and DMF (15 mL). Nitrogen was bubbled through the solution for 5 min, and then $Pd[P(Ph)_3]_4$ (693 mg, 0.6 mmol, 8 mol%) was added in one portion. The reaction mixture was stirred at 90 °C overnight. After cooling to room temperature, $NaHCO_3$ (aq, sat.) was added, and the mixture was extracted with $EtOAc$. The organic extracts were collected and dried with Na_2SO_4 . Evaporation of the solvent under reduced pressure and purification by column chromatography on silica gel (2% $MeOH/CH_2Cl_2$) afforded **27d** (900 mg, 84%) as a white solid. 1H NMR ($CDCl_3$,

300 MHz) 7.70 (1 H, d, $J = 1.8$ Hz), 7.55 (1 H, d, $J = 8.7$, 1.8 Hz), 6.78 (1 H, d, $J = 8.7$ Hz), 4.93 (1 H, bs). GC/MS (m/z %) 143 (M^+ , 100%), 116 ($M^+ - \text{HCN}$, 30%), R_t 14.4 min.

4-Amino-3-[6-(4-methylpiperazinyl)benzimidazol-2-yl]-2-oxo-hydroquinoline-6-carbonitrile (19ai). Method A (24% yield). ^1H NMR (300 MHz, $\text{DMSO}-d_6$) 11.61 (1 H, bs), 11.09 (1 H, s), 8.88 (1 H, d, $J = 1.5$ Hz), 7.95 (1 H, dd, $J = 8.7$, 1.5 Hz), 7.66 (1 H, d, $J = 8.7$ Hz), 7.47 (1 H, d, $J = 9.0$ Hz), 7.29 (1 H, s), 7.28 (1 H, d, $J = 9.0$ Hz), 3.82 (2 H, m), 3.52 (2 H, m), 3.29 (4 H, m), 2.80, (3 H, s). ^{13}C NMR (75 MHz, $\text{DMSO}-d_6$) 161.6, 153.8, 147.6, 146.7, 142.5, 135.3, 134.4, 130.4, 128.6, 119.5, 117.9, 116.9, 115.3, 113.7, 104.4, 101.2, 90.2, 52.5, 47.7, 42.5. LCMS (m/z) 400.4 (M^+), R_t 1.89 min.

4-Amino-3-[6-(4-methylpiperazinyl) benzimidazol-2-yl]-2-oxo-hydroquinoline-6-carboxylic acid (19aj). Compound 19ai (24 mg, 0.06 mmol, 1.0 equiv) was dissolved in a 1:1 mixture of EtOH and 30% aq NaOH (2 mL). The solution was heated to 100 °C for 2 h. The mixture was cooled to room temperature, concentrated, and neutralized with 1 N HCl. The precipitate was filtered and washed with H_2O twice and dried to afford the desired 19aj in quantitative yield. LCMS (m/z) 419.2 (M^+), R_t 1.35 min.

{4-Amino-3-[6-(4-methylpiperazinyl)benzimidazol-2-yl]-2-oxo(6-hydroquinolyl)}-N-benzylcarboxamide (19t). Compound 19aj (25 mg, 0.06 mmol, 1.0 equiv) was suspended in DMF (2 mL). Triethylamine (0.016 mL, 0.12 mmol, 2.0 equiv) and benzylamine (0.009 mL, 0.08 mmol, 1.2 equiv) were added, followed by EDC (16 mg, 0.08 mmol, 1.2 equiv) and HOAT (11 mg, 0.08 mmol, 1.2 equiv). The reaction mixture was stirred at room temperature for 2 days. Water was then added, and the mixture was extracted with EtOAc. The residue was purified by reverse phase HPLC to give 19t (13.8 mg, 45%). ^1H NMR (300 MHz, $\text{DMSO}-d_6$) 11.67 (1 H, s), 11.49 (1 H, bs), 9.42 (1 H, app. t, $J = 5.4$ Hz), 9.27 (1 H, s), 8.50 (1 H, bs), 8.11 (1 H, dd, $J = 8.4$, 1.2 Hz), 7.65 (1 H, d, $J = 9.6$ Hz), 7.4–7.1 (7 H, m), 4.49 (2 H, app d, $J = 5.7$ Hz), 3.82 (2 H, m), 3.51 (2 H, m), 3.24 (4 H, m), 2.80, (3 H, s). ^{13}C NMR (75 MHz, $\text{DMSO}-d_6$) 165.1, 161.1, 154.3, 147.2, 146.4, 140.8, 139.8, 133.5, 131.4, 128.2, 127.4, 127.2, 126.7, 124.1, 116.0, 115.8, 114.5, 112.1, 100.2, 88.9, 52.0, 46.9, 42.6, 41.9. LCMS (m/z) 508.5 (M^+), R_t 2.11 min.

4-Amino-7-fluoro-3-[6-(4-methylpiperazinyl)benzimidazol-2-yl]hydroquinolin-2-one (19u). Method A (46% yield). ^1H NMR (300 MHz, $\text{DMSO}-d_6$) 11.45 (1 H, s), 9.9 (1 H, bs), 8.25 (1 H, dd, $J = 8.8$, 5.8 Hz), 7.55 (1 H, d, $J = 8.8$ Hz), 7.38 (1 H, s), 7.1 (2 H, m), 6.95 (1 H, dd, $J = 2.1$, 8.8 Hz), 3.75 (1 H, m), 3.55 (1 H, m), 3.24 (1 H, m) 3.0 (1 H, m), 2.9 (3 H, s). ^{13}C NMR (75 MHz, $\text{DMSO}-d_6$) 166.5, 163.2, 161.8, 154.5, 147.8, 147.5, 141.5, 134.3, 127.9, 127.7, 116.6, 115.1. HRMS found m/z 393.1811; $\text{C}_{21}\text{H}_{22}\text{N}_6\text{OF}$ requires 393.1833.

4-Amino-7-(methylamino)-3-[6-(4-methylpiperazinyl)benzimidazol-2-yl]hydroquinolin-2-one (19v). Compound 19u (28 mg, 0.07 mmol, 1.0 equiv) was combined with MeNH_2 (8 M) and 1:1 EtOH:NMP (2 mL) and then heated under microwave irradiation 4 times for 5 min at 220 °C. After cooling, water was added and the mixture extracted with EtOAc. The organic extracts were collected and dried over Na_2SO_4 . Evaporation of the solvent under reduced pressure, and purification of the residue by reverse phase HPLC afforded 19v (7.1 mg, 21%). ^1H NMR (300 MHz, $\text{DMSO}-d_6$) 11.64 (1 H, bs, NH), 11.11 (1 H, s, NH), 7.99 (1 H, d, $J = 9.0$ Hz), 7.62 (1 H, d, $J = 9.6$ Hz), 7.23 (1 H, d, $J = 9.6$ Hz), 7.22 (1 H, s), 6.56 (1 H, dd, $J = 9.0$, 1.8 Hz), 6.32 (1 H, d, $J = 8.1$, 1.8 Hz), 3.79 (2 H, m), 3.50 (2 H, m), 3.24 (4 H, m), 2.79 (3 H, bs), 2.72 (3 H, s). ^{13}C NMR (75 MHz, $\text{DMSO}-d_6$) 162.9, 155.3, 153.5, 148.1, 147.1, 142.2, 133.1, 126.8, 125.8, 116.7, 110.8, 103.2, 100.5, 94.9, 85.7, 52.6, 47.4, 42.5, 30.1. LCMS (m/z) 404.4 (M^+), R_t 1.72 min. HRMS found m/z 404.2189; $\text{C}_{22}\text{H}_{26}\text{N}_7\text{O}$ requires 404.2193.

2-Amino-3-fluorobenzonitrile (17a).³⁷ 2,3-Difluorobenzonitrile (2.0 g, 14.4 mmol, 1 equiv) was dissolved in anhydrous EtOH (25 mL) in a glass pressure vessel. The solution was saturated with gaseous NH_3 , and the vessel was sealed. The reaction mixture was stirred at 140 °C for 3 days and then cooled to room temperature. Evaporation of the solvent under reduced pressure and purification

of the residue by chromatography (3:1 EtOAc:hexanes) on silica gel afforded 17a (1.0 g, 51%). GC/MS (m/z %) 136 (M^+ , 100%), 109 ($M^+ - \text{HCN}$, 30%) R_t 7.93 min.

4-Amino-8-fluoro-3-[6-(4-methylpiperazinyl)benzimidazol-2-yl]hydroquinolin-2-one (19w). Method A (45% yield). ^1H NMR (300 MHz, $\text{DMSO}-d_6$) 11.40 (1 H, s, NH) 8.61 (1 H, bs, NH), 8.1 (1 H, d, $J_{\text{H-H}} = 8.4$ Hz), 7.64 (1 H, d, $J_{\text{H-H}} = 9.0$ Hz), 7.51 (1 H, dd, $J_{\text{H-F}} = 10.7$, $J_{\text{H-H}} = 7.8$ Hz), 7.26 (1 H, d, $J_{\text{H-H}} = 2.1$ Hz), 7.21 (1 H, dd, $J_{\text{H-H}} = 9.0$, 2.1 Hz), 7.20 (1 H, ddd, $J_{\text{H-H}} = 8.4$, 7.8, $J_{\text{H-F}} = 3.0$ Hz), 3.80 (2 H, m), 3.51 (2 H, m), 3.22 (4 H, m), 2.8 (3 H, s). ^{13}C NMR (75 MHz, $\text{DMSO}-d_6$) 161.7, 154.1, 149.9 (d, $J_{\text{C-F}} = 244.0$ Hz, C ipso), 147.7, 135.8, 135.0, 128.4 (d, $J_{\text{C-F}} = 14.5$ Hz), 121.9, 120.3, 117.8, 116.3, 115.7, 115.3, 100.8, 90.4, 52.8, 47.6, 42.5. LCMS (m/z) 393.1 (M^+), R_t 1.48 min. HPLC R_t 14.96 min. HRMS found m/z 393.1802; $\text{C}_{21}\text{H}_{22}\text{N}_6\text{OF}$ requires 393.1833.

4-Amino-6,7-difluoro-3-(6-(4-methylpiperazin-1-yl)-1H-benzimidazol-2-yl)quinolin-2(1H)-one (19x). Synthesized via modified isatoic anhydride route as previously described.¹⁸ (28% yield for 3 steps). LCMS (m/z) 411.3 (M^+), R_t 1.82 min.

6-Amino-2,4-difluorobenzonitrile (17b).³⁸ 2,4,6-Trifluorobenzonitrile (160 mg, 1 mmol, 1.0 equiv) was dissolved in CH_3CN and conc NH_4OH (2:1, 6 mL). The reaction mixture was stirred at room temperature for 3 days. The reaction mixture was then diluted with CH_2Cl_2 . The organic phase was washed with H_2O , brine, and then dried with Na_2SO_4 . Evaporation of the solvent under reduced pressure afforded a mixture of 2-amino-4,6-difluorobenzonitrile (17b) and 4-amino-2,6-difluorobenzonitrile. The two isomers were separated by flash chromatography on silica gel (1:2 EtOAc:hexanes) and the desired 2-amino-4,6-difluorobenzonitrile (17b) in 47% yield (72 mg). ^1H NMR (300 MHz, CDCl_3) 6.25 (1H, ddd, $J_{\text{H-F}} = 10.8$, 9.9, $J_{\text{H-H}} = 2.1$ Hz) 6.23 (1H, dd, $J_{\text{H-F}} = 10.7$, $J_{\text{H-H}} = 2.1$ Hz); GC/MS (m/z %) 154 (M^+ , 100%).

4-Amino-5,7-difluoro-3-[6-(4-methylpiperazinyl)benzimidazol-2-yl]hydroquinolin-2-one (19y). Method A (45% yield). ^1H NMR (CDCl_3 , 300 MHz): 11.75 (1 H, s, NH), 11.50 (1 H, bs, NH), 7.56 (1 H, d, $J_{\text{H-H}} = 9.0$ Hz), 7.37 (1 H, dd, $J_{\text{H-F}} = 11.4$, $J_{\text{H-H}} = 2.1$ Hz), 7.26 (1 H, d, $J_{\text{H-H}} = 1.8$ Hz), 7.14 (1 H, ddd, $J_{\text{H-F}} = 11.4$, 9.0, $J_{\text{H-H}} = 2.1$ Hz), 7.03 (1 H, dd, $J_{\text{H-H}} = 9.0$, 1.8 Hz), 3.73 (2 H, m), 3.48 (2 H, m), 3.20 (4 H, m), 2.78 (3 H, s). LCMS (m/z) 411.2 (M^+), R_t 1.94 min.

4-Amino-7-(dimethylamino)-6-fluoro-3-(6-(4-methylpiperazin-1-yl)-1H-benzimidazol-2-yl)quinolin-2(1H)-one (19z). Compound 19x (0.0569 mg, 0.14 mmol, 1.0 equiv) and Me_2NH (2 M in THF, 1.0 mL, 2.0 mmol, 13.3 equiv) were heated in NMP (2 mL) at 80 °C overnight. After cooling, the reaction mixture was purified by reverse phase HPLC to afford 19z (38.7 mg, 47% yield). LCMS (m/z) 436.2 (M^+), R_t 1.85 min. HRMS found m/z 436.2274; $\text{C}_{23}\text{H}_{27}\text{N}_7\text{OF}$ requires 436.2255.

2-(4-Methylpiperazinyl)-6-nitrobenzenecarbonitrile.²¹ Yield 69%. ^1H NMR (300 MHz, $\text{DMSO}-d_6$) 7.83 (1 H, dd, $J = 8.1$, 1.2 Hz), 7.78 (1 H, t, $J = 8.1$ Hz), 7.58 (1 H, dd, $J = 8.1$, 1.2 Hz), 3.23 (4 H, t, $J = 4.8$ Hz), 2.49 (4 H, t, $J = 4.8$ Hz), 2.22 (3 H, s). ^{13}C NMR (75 MHz, $\text{DMSO}-d_6$) 157.7 (C), 150.4 (C), 134.3 (CH), 125.3 (CH), 117.8 (CH), 114.2 (C), 98.7 (C), 54.4 (CH_2), 51.2 (CH_2), 45.6 (CH_3). LCMS m/z 247.2 (M^+), R_t 1.64 min. Anal. calcd for $\text{C}_{12}\text{H}_{14}\text{N}_4\text{O}_2$: C, 58.53; H, 5.73; N, 22.75; found: C, 58.60; H, 5.74, N, 22.62.

6-Amino-2-(4-methylpiperazinyl)benzenecarbonitrile (27a).²¹ Yield 28%. ^1H NMR (300 MHz, $\text{DMSO}-d_6$) 7.14 (1 H, t, $J = 8.2$ Hz), 6.38 (1 H, dd, $J = 8.2$, 0.9 Hz), 6.19 (1 H, dd, $J = 8.2$, 0.9 Hz), 3.02 (4 H, t, $J = 4.5$ Hz), 2.46 (4 H, t, $J = 4.5$ Hz), 2.22 (3 H, s). ^{13}C NMR (75 MHz, $\text{DMSO}-d_6$) 156.1 (C), 153.2 (C), 134.0 (CH), 117.3 (C), 108.8 (CH), 105.2 (CH), 88.5 (C), 54.7 (CH_2), 51.2 (CH_2), 45.7 (CH_3). LCMS m/z 217.4 (M^+), R_t 0.99 min. Anal. calcd for $\text{C}_{12}\text{H}_{16}\text{N}_4$: C, 66.64; H, 7.46; N, 25.90; found: C, 66.68; H, 7.40, N, 25.90.

4-Amino-3-benzimidazol-2-yl-5-(4-methylpiperazinyl)hydroquinolin-2-one (19aa). Method A (15% yield). ^1H NMR (300 MHz, $\text{DMSO}-d_6$) 11.47 (2 H, s), 9.70 (2 H, bs), 7.72 (2 H, dd, $J = 6.0$, 3.3 Hz), 7.55 (1 H, t, $J = 8.0$ Hz), 7.34 (2 H, dd, $J = 6.0$, 3.3 Hz),

7.20 (1 H, d, $J = 8.0$ Hz), 7.06 (1 H, d, $J = 8.0$ Hz), 4.80 (6 H, bs), 3.41 (8 H, m), 2.83 (3 H, d, $J = 4.2$ Hz). ^{13}C NMR (75 MHz, DMSO- d_6) 160.7 (C), 156.1 (C), 150.4 (C), 149.0 (C), 140.5 (C), 133.8 (C), 132.5 (CH), 123.3 (CH), 113.7 (CH), 113.5 (CH), 106.5 (C), 88.9 (C), 52.2 (CH₂), 50.2 (CH₂), 42.2 (CH₃). LCMS m/z 375.4 (MH⁺), R_t 1.74 min. HRMS found m/z 375.1897; C₂₁H₂₃N₆O requires 375.1927.

6-Amino-2-(1-methyl(3-piperidyloxy))benzenecarbonitrile (27b). 3-Hydroxy-1-methylpiperidine (4.1 mL, 35.6 mmol) was added dropwise to hexane-washed NaH (1.03 g, 43.0 mmol) in NMP (30 mL). After 15 min, 2-amino-6-fluorobenzonitrile (4.03 g, 29.6 mmol) was added in portions. The reaction mixture was heated to 100 °C for 2 h. The reaction mixture was poured into H₂O and extracted with EtOAc (2×). The combined organic layers were washed with H₂O (3×) and brine. The organic layer was dried with Na₂SO₄, filtered, and concentrated. The crude material was purified by column chromatography on silica gel (50% EtOAc/hex to EtOAc to 5% MeOH/1% Et₃N/94% CH₂Cl₂) to give **27b** (3.31 g, 49% yield) as a brown solid. ^1H NMR (300 MHz, DMSO- d_6) 7.13 (1 H, t, $J = 8.4$ Hz), 6.31 (1 H, d, $J = 8.4$ Hz), 6.24 (1 H, d, $J = 8.4$ Hz), 5.93 (2 H, s), 4.36 (1 H, sept, $J = 4.5$ Hz), 2.80 (1 H, m), 2.49 (1 H, m), 2.14 (3 H, s), 1.98 (3 H, m), 1.69 (1 H, m), 1.51 (1 H, m), 1.25 (1 H, m). ^{13}C NMR (75 MHz, DMSO- d_6) 159.6 (C), 153.1 (C), 134.3 (CH), 115.6 (C), 107.3 (CH), 99.8 (CH), 85.4 (C), 73.0 (CH), 59.0 (CH₂), 54.7 (CH₂), 45.9 (CH₃), 29.0 (CH₂), 22.4 (CH₂). LCMS m/z 232.3 (MH⁺), R_t 1.47 min.

4-Amino-3-benzimidazol-2-yl-5-(1-methyl(3-piperidyloxy))hydroquinolin-2-one (19ab). Method A (8% yield). ^1H NMR (300 MHz, DMSO- d_6) 11.55 (1H, bs), 11.50 (1 H, s), 11.43 (1 H, s), 10.57 (1 H, bs), 8.90 (2 H, bs), 7.73 (2 H, p, $J = 3.3$ Hz), 7.51 (1 H, dt, $J = 8.4, 1.8$ Hz), 7.36 (2 H, p, $J = 3.3$ Hz), 7.04 (1 H, d, $J = 8.4$ Hz), 6.97 (1 H, dd, $J = 24.3, 8.4$ Hz), 5.15 (1 H, bs), 4.90 (4 H, bs), 3.79 (1 H, m), 3.21 (3 H, m), 2.80 (3 H, s), 2.07 (4 H, m). ^{13}C NMR of HCl salt (75 MHz, DMSO- d_6) 160.8 (C), 156.1/156.0 (C), 155.7/155.5 (C), 148.5/148.4 (C), 141.0/140.8 (C), 133.8/133.1 (CH), 123.5 (CH), 113.9 (CH), 109.9/109.5 (CH), 106.2/105.9 (CH), 103.9/103.3 (C), 88.5/87.6 (C), 71.7 (CH), 54.1/52.6 (CH₂), 43.1/42.6 (CH₃), 27.3/25.4 (CH₂), 20.3/18.2 (CH₂). LCMS m/z 390.4 (MH⁺), R_t 1.98 min. HRMS found m/z 390.1900; C₂₂H₂₄N₅O₂ requires 390.1924. Anal. calcd for C₂₂H₂₃N₅O₂: C, 67.85; H, 5.95; N, 17.98; found: C, 67.48; H, 6.01; N, 17.78.

5-(4-Methylpiperazinyl)-2-nitrobenzenecarbonitrile.²² Yield 95%. ^1H NMR (300 MHz, DMSO- d_6) 8.15 (1 H, d, $J = 8.2$ Hz), 7.52 (1 H, d, $J = 2.1$ Hz), 7.24 (1 H, dd, $J = 8.2, 2.1$ Hz), 3.53 (4 H, m), 2.41 (4 H, m), 2.21 (3 H, s). ^{13}C NMR (75 MHz, DMSO- d_6) 153.4 (C), 135.5 (C), 127.9 (CH), 118.9 (CH), 116.2 (C), 115.5 (CH), 109.1 (C), 54.0 (CH₂), 46.2 (CH₂), 45.5 (CH₃). LCMS m/z 247.3 (MH⁺), R_t 1.62 min.

2-Amino-5-(4-methylpiperazinyl)benzenecarbonitrile (27c).²² Yield 91%. ^1H NMR (300 MHz, DMSO- d_6) 7.07 (1 H, dd, $J = 9.0, 2.7$ Hz), 6.84 (1 H, d, $J = 2.7$ Hz), 6.75 (1 H, d, $J = 9.0$ Hz), 2.92 (4 H, t, $J = 4.8$ Hz), 2.40 (4 H, t, $J = 4.8$ Hz), 2.18 (3 H, s). ^{13}C NMR (75 MHz, DMSO- d_6) 145.7 (C), 142.1 (C), 125.1 (CH), 118.5 (C), 117.7 (CH), 116.7 (CH), 93.7 (C), 54.7 (CH₂), 49.5 (CH₂), 45.7 (CH₃). LCMS m/z 217.4 (MH⁺), R_t 0.70 min.

4-Amino-3-benzimidazol-2-yl-6-(4-methylpiperazinyl)hydroquinolin-2-one (19ac). Method A (1% Yield). LCMS m/z 375.4 (MH⁺), R_t 1.87 min. HRMS found m/z 375.1909; C₂₁H₂₃N₆O requires 375.1927.

Molecular Modeling. The VEGFR-2 homology model was built using Chemical Computing Group's MOE software. Default settings were used in the alignment and homology modeling module and the FGFR-1 crystal structure 2FGI from the Brookhaven Protein Data Bank was used as a template. The model was brought into Maestro (version 8.0.308, Schrödinger LLC) and aligned with the CHK-1 crystal structure of the 6-Cl analogue of **16c** (PDB code 2GDO).¹⁸ The 4-amino-3-benzimidazol-2-ylhydroquinolin-2-one core was extracted from the CHK-1 structure and placed into the aligned active site of the VEGFR-2 homology model. The complex was prepared for Prime optimization using the Protein Preparation Wizard in Maestro (fixing bond orders, adding hydro-

gens, optimizing hydrogen bonds, optimizing hydrogens). A Prime optimization (Prime version 1.6) was performed on the core and the residues in a 6 Å sphere around it, resulting in a binding pose of the core with 3 hydrogen bonds to the hinge region (to Glu917-CO, Cys919-NH, Cys919-CO). A Glide grid was subsequently created using default settings (Glide version 45208) around the optimized core, and used to dock ligands like **5**, after creating their input conformations through LigPrep (version 21207) and using SP precision (GlideScore version SP4.5).

In Vitro Kinase Assays. FGFR-1, PDGFR β , and VEGFR-2 receptor tyrosine kinases used in isolated enzyme assays were purified from insect cell lysates that were infected with recombinant baculovirus containing the respective human kinase domains. All kinases contained the wild type amino acid sequence.

The IC₅₀ values for the inhibition of RTKs were determined in the Alpha Screen format by measuring the inhibition by compound of phosphate transfer to a peptide substrate by the respective enzyme. Briefly, the respective RTK cytosolic domain was purchased as human recombinant protein (VEGFR-2, Invitrogen no. PV3660, PDGFR β Invitrogen no. P3082, and FGFR-1 Upstate 14-582) were incubated with serial dilutions of compound in the presence of peptide substrate and ATP at concentrations at or below the $K_{m(\text{app})}$ of ATP.

The kinase domain of FGFR-1 was assayed in 50 mM Hepes, pH 7.5, 2 mM MgCl₂, 5 mM MnCl₂, 1 mM DTT, 0.1% BSA with 0.2 μM biotinylated peptide substrate (b-GGGGQDGKDYIVLPI-NH₂), VEGFR-2 in 50 mM Hepes, pH 7.5, 5 mM MnCl₂, 0.1%BSA, 0.01%Tween-20, 1 mM DTT, and 1 μM of the same biotinylated substrate and PDGFR β in 50 mM Hepes, pH 7.5, 20 mM MgCl₂, 1 mM DTT, 0.1% BSA with 0.1 μM biotinylated peptide substrate (b-GGLFDDPSYVNVQNL-NH₂) at ATP concentrations of 5, 1, and 10 μM , respectively, depending on the ATP $K_{m(\text{app})}$ for the respective enzyme. Reactions were incubated at room temperature for 2.5 h and then stopped with buffer (70 mM Tris, pH 7.5, 17.1 mM EDTA, 0.011% Tween-20 for PDGFR β and FGFR-1; 50 mM Hepes, pH 7.5, 60 mM EDTA, 0.1% BSA, 0.01% Tween-20 for VEGFR-2). Next the stopped reactions were incubated with PY20 Ab/Alpha Screen IgG beads overnight and then read on an Alpha Screen reader. The concentration of compound for 50% inhibition (IC₅₀) was calculated by employing nonlinear regression using XL-Fit data analysis software and represents the average of at least 2 experiments. As a control compound, staurosporine is run on every assay plate. Additionally, a $Z' > 0.5$ is required to validate results for each plate.

Cell Proliferation Assays. HMVECs (human microvascular endothelial cells) were purchased from Clonetics (San Diego, CA). Cells were grown as monolayers in media (EBM-2MV from Clonetics) and maintained at 37 °C in a humidified atmosphere with 5% CO₂. To perform the VEGF-mediated proliferation assay, cells were seeded in 96-well plates at 2000 cells per well in assay medium (EBM-2 with 5% FBS). The following day, serial dilutions of compound at 0.2% final DMSO concentration in assay medium with 2.5 ng/mL of VEGF were added to the cells. Control wells contained cells in assay medium without the VEGF. After 72 h, the number of viable cells left was determined using the CellTiter-Glo assay (Promega, Madison, WI) as described by the manufacturer. Plates were read on a luminometer. The IC₅₀ values were calculated using nonlinear regression using XL Fit data analysis software and represent the average of two experiments.

Cell Lines. Human colon tumor cell lines (KM12L4A), prostate (DU145), and acute myelogenous leukemia (AML) FLT-3 ITD cell line (MV4;11) were obtained from American Tissue Culture Collection (Rockville, MD). KM12L4A, or DU145, cells were cultured in RPMI 1640 (Life Technologies, Gaithersburg, MD) supplemented with 10% fetal bovine serum (FBS) and 1% L-glutamine. MV4;11 cells were grown in Iscoves modified Dulbecco medium (IMBM) supplemented with 10% fetal bovine serum (FBS, Gibco Life Technologies, Gaithersburg, MD) containing 4 mM L-glutamine, 5 ng/mL granulocyte-macrophage colony stimulating factor (GM-CSF, R&D Systems, Minneapolis, MN), and 1% penicillin and streptomycin. Cells were grown as adherent or

suspension cultures and maintained in a humidified atmosphere at 37 °C and 5% CO₂. Cells were used in exponential growth phase, with viability >98% (assessed using trypan blue staining) and determined free of mycoplasma.

In Vivo bFGF-Mediated Matrigel Angiogenesis Assays. A mixture of 0.5 mL of Matrigel (Becton Dickinson, Bedford, MA) with 2 µg of bFGF (Chiron Corporation; Emeryville, CA) was implanted subcutaneously into female BDF1 mice (Charles River, Wilmington, MA). Vehicle or doses of **5** (HCl salt, formulated in 5 mM citrate) ranging from 0 to 200 mg/kg/d was given daily via oral gavage for 8 days. On day 8, 4 h post dose, Matrigel plugs were removed and homogenized in 0.5 mL deionized water using a Polytron homogenizer (Kinematica Littau, Switzerland). Hemoglobin content in Matrigel plugs was quantified by a colorimetric assay using Drabkin's procedure (Hemoglobin Test Kit, Sigma Diagnostics, St. Louis, MO).

In Vivo Tumor Efficacy Studies. Nude (nu/nu) or SCID-NOD mice (6–8 week-old, 18–22 g) were obtained from Charles River (Wilmington, MA) and acclimated for 1 week in a pathogen-free enclosure prior to the start of the study. MV4;11 cells (5×10^6 cells/mouse) were reconstituted with 50% Matrigel (Becton Dickinson) and implanted sc into the right flank of SCID-NOD mice. KM12L4A (2×10^6 cells) were implanted subcutaneously into the flank of female nude mice. DU145 tumor pieces (2 mm \times 2 mm) from a passaged DU145 tumor (500 mm³) were implanted subcutaneously using a trocar into male nude mice. Tumors were allowed to grow to a size of approximately 200–500 mm³ prior to initiation of drug treatment. Mice were randomly assigned into cohorts (typically 10 mice/group) and treated with either vehicle or **5** (10–100 mg/kg/d) once daily by oral gavage. Tumor volumes and body weights were assessed 2–3 times weekly. Caliper measurements of tumors were converted into mean tumor volume (mm³) using the formula: $\frac{1}{2} (\text{length (mm)} \times [\text{width (mm)}]^2)$. Percent tumor growth inhibition (TGI) was determined as $[1 - (\text{mean tumor volume of each } \mathbf{5}\text{-treated dose group} / \text{mean tumor volume of vehicle-treated group})] \times 100$. Statistical analyses: Student's *t* test was used to measure statistical significance between two treatment groups. Multiple comparisons were done using one-way analysis of variance (ANOVA), and post-tests comparing different treatment means were done using either Student–Newman–Keuls or Dunn's test (SigmaStat, San Rafael, CA). Differences were considered statistically significant at *p* < 0.05.

Acknowledgment. We thank Lara Nordhal and Yan Tang for their excellent technical expertise with the in vivo studies, and Weiping Jia, Keshi Wang, and Dazhi Tang for their analytical support.

Supporting Information Available: Elemental analysis data or high resolution mass spectrometry data for key compounds, MS, HPLC traces, and ¹H NMR for **5**. This material is available free of charge via the Internet at <http://pubs.acs.org>.

References

- Folkman, J.; Merler, E.; Abernathy, C.; Williams, G. Isolation of a tumor factor responsible for angiogenesis. *J. Exp. Med.* **1971**, *133* (2), 275–288.
- Carmeliet, P. Mechanisms of angiogenesis and arteriogenesis. *Nat. Med.* **2000**, *6* (4), 389–395.
- Penault-Llorca, F.; Bertucci, F.; Adelaiede, J.; Parc, P.; Coulier, F.; Jacquemier, J.; Birnbaum, D.; DeLapeyriere, O. Expression of FGF and FGF receptor genes in human breast cancer. *Int. J. Cancer* **1995**, *61* (2), 170–176.
- Kyzas, P. A.; Stefanou, D.; Batistatou, A.; Agnantis, N. J. Potential autocrine function of vascular endothelial growth factor in head and neck cancer via vascular endothelial growth factor receptor-2. *Mod. Pathol.* **2005**, *18* (4), 485–494.
- Oestman, A. PDGF receptors-mediators of autocrine tumor growth and regulators of tumor vasculature and stroma. *Cytokine Growth Factor Rev.* **2004**, *15* (4), 275–286.
- Patel, P. H.; Chaganti, R. S.; Motzer, R. J. Targeted therapy for metastatic renal cell carcinoma. *Br. J. Cancer* **2006**, *94* (5), 614–619.
- Liao, J. J.-L. Molecular Recognition of Protein Kinase Binding Pockets for Design of Potent and Selective Kinase Inhibitors. *J. Med. Chem.* **2007**, *50* (3), 409–424.
- Albert, D. H.; Tapang, P.; Magoc, T. J.; Pease, L. J.; Reuter, D. R.; Wei, R.-Q.; Li, J.; Guo, J.; Bousquet, P. F.; Ghoreishi-Haack, N. S.; Wang, B.; Bukofzer, G. T.; Wang, Y.-C.; Stavropoulos, J. A.; Hartandi, K.; Niquette, A. L.; Soni, N.; Johnson, E. F.; McCall, J. O.; Bouska, J. J.; Luo, Y.; Donawho, C. K.; Dai, Y.; Marcotte, P. A.; Glaser, K. B.; Michaelides, M. R.; Davidsen, S. K. Preclinical activity of ABT-869, a multitargeted receptor tyrosine kinase inhibitor. *Mol. Cancer Ther.* **2006**, *5* (4), 995–1006.
- George, D. J. Phase 2 Studies of Sunitinib and AG013736 in Patients with Cytokine-Refractory Renal Cell Carcinoma. *Clin. Cancer Res.* **2007**, *13* (2, Pt. 2), 753s–757s.
- Lee, S. H.; Lopes de Menezes, D.; Vora, J.; Harris, A.; Ye, H.; Nordahl, L.; Garrett, E.; Samara, E.; Aukerman, S. L.; Gelb, A. B.; Heise, C. In Vivo Target Modulation and Biological Activity of CHIR-258, a Multitargeted Growth Factor Receptor Kinase Inhibitor, in Colon Cancer Models. *Clin. Cancer Res.* **2005**, *11* (10), 3633–3641.
- Lopes de Menezes, D. E.; Peng, J.; Garrett, E. N.; Louie, S. G.; Lee, S. H.; Wiesmann, M.; Tang, Y.; Shephard, L.; Goldbeck, C.; Oei, Y.; Ye, H.; Aukerman, S. L.; Heise, C. CHIR-258: A Potent Inhibitor of FLT3 Kinase in Experimental Tumor Xenograft Models of Human Acute Myelogenous Leukemia. *Clin. Cancer Res.* **2005**, *11* (14), 5281–5291.
- Trudel, S.; Li, Z. H.; Wei, E.; Wiesmann, M.; Chang, H.; Chen, C.; Reece, D.; Heise, C.; Stewart, A. K. CHIR-258, a novel, multitargeted tyrosine kinase inhibitor for the potential treatment of t(4;14) multiple myeloma. *Blood* **2005**, *105* (7), 2941–2948.
- Ukrainets, I. V.; Bezuglyi, P. A.; Treskach, V. I.; Turov, A. V. 2-(Carbomethoxymethyl)-4H-3,1-benzoxazin-4-one. 3. Condensation with *o*-phenylenediamine. *Khim. Geterotsikl. Soedin.* **1992**, (2), 239–241.
- Ukrainets, I. V.; Taran, S. G.; Turov, A. V. 4-Hydroxy-2-quinolones. 16. Condensation of 2-carboxymalonanilic acid *N*-*R*-substituted amides with *o*-phenylenediamine. *Khim. Geterotsikl. Soedin.* **1993**, (8), 1105–1108.
- Ukrainets, I. V.; Bezugly, P. A.; Taran, S. G.; Gorokhova, O. V.; Turov, A. V. Effective Synthesis of 3-(Benzimidazol-2-yl)-4-hydroxy-2-oxo-1,2-dihydroquinolines. *Tetrahedron Lett.* **1995**, *36* (42), 7747–7748.
- Ukrainets, I. V.; Bezugly, P. A.; Gorokhova, O. V.; Treskach, V. I.; Turov, A. V. 4-Hydroxy-2-quinolones. 7. Synthesis and biological properties of 1-*R*-3-(benzimidazolyl)-2-4-hydroxy-2-quinolones. *Khim. Geterotsikl. Soedin.* **1993**, (1), 105–108.
- Matei, S.; Russu, J.; Coltea, P.; Grecu, R. Condensation of ethyl 2-benzimidazoleacetate with carbonyl compounds. *Rev. Chim. (Bucharest, Rom.)* **1982**, *33* (6), 527–530.
- Ni, Z.-J.; Barsanti, P.; Brammeier, N.; Diebes, A.; Poon, D. J.; Ng, S.; Pecchi, S.; Pfister, K.; Renhowe, P. A.; Ramurthy, S.; Wagman, A. S.; Bussiere, D. E.; Le, V.; Zhou, Y.; Jansen, J. M.; Ma, S.; Gesner, T. G. 4-(Aminoalkylamino)-3-benzimidazole-quinolinones as potent CHK-1 inhibitors. *Bioorg. Med. Chem. Lett.* **2006**, *16* (12), 3121–3124.
- Antonios-McCrea, W. R.; Frazier, K. A.; Jazan, E. M.; Machajewski, T. D.; McBride, C. M.; Pecchi, S.; Renhowe, P. A.; Shafer, C. M.; Taylor, C. LHMS mediated tandem acylation-cyclization of 2-amino-benzenecarbonitriles with 2-benzimidazol-2-yl acetates: a short and efficient route to the synthesis of 4-amino-3-benzimidazol-2-ylhydroquinolin-2-ones. *Tetrahedron Lett.* **2006**, *47* (5), 657–660.
- Church, T. J.; Cutshall, N. S.; Gangloff, A. R.; Jenkins, T. E.; Linsell, M. S.; Litvak, J.; Rice, K. D.; Spencer, J. R.; Wang, V. R. Preparation of compounds and compositions for treating diseases associated with serine protease, particularly trypsin, activity Patent 9845275, 1998.
- Klauber, D. H.; Sellstedt, J. H.; Guinasso, C. J.; Capetola, R. J.; Bell, S. C. *N*-(Aminophenyl)oxamic acids and esters as potent, orally active antiallergy agents. *J. Med. Chem.* **1981**, *24* (6), 742–748.
- Elslager, E. F.; Clarke, J.; Werbel, L. M.; Worth, D. F.; Davoll, J. Antimalarial drugs. 25. Folate antagonists. 3. 2,4-Diamino-6-(heterocyclic)quinazolines, a novel class of antimetabolites with potent antimalarial and antibacterial activity. *J. Med. Chem.* **1972**, *15* (8), 827–836.
- At pH 7, the solubility of **8c** was <0.030 µg/mL while the solubility of **16c** was 107 µg/mL.
- Unpublished results.
- Knight, Z. A.; Shokat, K. M. Features of Selective Kinase Inhibitors. *Chem. Biol.* **2005**, *12* (6), 621–637.
- Wiesmann, M.; Lee, S. H.; LaPointe, G.; Javandel, M.; Heise, C.; Renhowe, P.; Wernette-Hammond, M.-E.; Gesner, T.; Harrison, S.;

- Harris, A. L. In *In Vitro Characterization of a Potent Tyrosine Kinase Inhibitor, CHIR258, That Modulates Angiogenesis and Proliferation of Selected Cancer Cell Lines*, American Association of Cancer Research: Washington, DC, 2003.
- (27) Additional modeling information can be found in the Supporting Information.
- (28) Cowan-Jacob, S. W. Structural biology of protein tyrosine kinases. *Cell. Mol. Life Sci.* **2006**, *63* (22), 2608–2625.
- (29) Vogtherr, M.; Saxena, K.; Hoelder, S.; Grimme, S.; Betz, M.; Schieborr, U.; Pescatore, B.; Robin, M.; Delarbre, L.; Langer, T.; Wendt, K. U.; Schwalbe, H. NMR characterization of kinase p38 dynamics in free and ligand-bound forms. *Angew. Chem., Int. Ed.* **2006**, *45* (6), 993–997.
- (30) Furet, P.; Bold, G.; Meyer, T.; Roesel, J.; Guagnano, V. Aromatic Interactions with Phenylalanine 691 and Cysteine 828: A Concept for FMS-like Tyrosine Kinase-3 Inhibition. Application to the Discovery of a New Class of Potential Antileukemia Agents. *J. Med. Chem.* **2006**, *49* (15), 4451–4454.
- (31) Compound **5** was analyzed in plasma using a qualified LC/MS/MS method with a calibration range of 1–8000 ng/mL, as described previously (Lee, S. H. et al. *Clin. Cancer Res.* **2005**, *11*, 3633–3641). Average concentration–time data was subject to PK analyses using standard noncompartmental methods using WinNonlin software (Pharsight Corporation, Mountain View, CA).
- (32) Harris, N. V.; Smith, C.; Bowden, K. Antifolate and antibacterial activities of 6-substituted 2,4-diaminoquinazolines. *Eur. J. Med. Chem.* **1992**, *27* (1), 7–18.
- (33) Rampa, A.; Bisi, A.; Belluti, F.; Gobbi, S.; Valenti, P.; Andrisano, V.; Cavrini, V.; Cavalli, A.; Recanatini, M. Acetylcholinesterase inhibitors for potential use in Alzheimer's disease: molecular modeling, synthesis and kinetic evaluation of 11*H*-indeno-[1,2-*b*]-quinolin-10-ylamine derivatives. *Bioorg. Med. Chem.* **2000**, *8* (3), 497–506.
- (34) Badawey, E. S. A. M.; Rida, S. M.; Soliman, F. S. G.; Kappe, T. Benzimidazole condensed ring systems. 4. New approaches to the synthesis of substituted pyrimido[1,6-*a*]benzimidazole-1,3(2*H*,5*H*)-diones. *J. Heterocycl. Chem.* **1989**, *26* (2), 405–408.
- (35) Self, D. P.; West, D. E.; Stillings, M. R. Cine and tele substitutions in the reaction of 2,3-dinitroaniline with secondary amines. *J. Chem. Soc., Chem. Commun.* **1980**, (6), 281–282.
- (36) Crosby, J.; Moilliet, J.; Parratt, J. S.; Turner, N. J. Regioselective hydrolysis of aromatic dinitriles using a whole cell catalyst. *J. Chem. Soc., Perkin Trans. 1* **1994**, *13*, 1679–1687, 1972–1999.
- (37) Adachi, M.; Sugawara, T. Exclusive ortho cyanation and alkylthio-carbonylation of anilines and phenols using boron trichloride. *Synth. Commun.* **1990**, *20* (1), 71–84.
- (38) Camps, P.; El Achab, R.; Morral, J.; Munoz-Torrero, D.; Badia, A.; Banos, J. E.; Vivas, N. M.; Barril, X.; Orozco, M.; Luque, F. J. New tacrine-huperzine A hybrids (huprines): highly potent tight-binding acetylcholinesterase inhibitors of interest for the treatment of Alzheimer's disease. *J. Med. Chem.* **2000**, *43* (24), 4657–4666.

JM800790T